A multiscale mathematical model describing the growth and development of bambara groundnut

Journal of Theoretical Biology 560 (2023) 111373

Contents lists available at ScienceDirect

Journal of Theoretical Biology

journal homepage: www.elsevier.com/locate/yjtbi

A multiscale mathematical model describing the growth and development of bambara groundnut

Josie Dodd [a], Peter K. Sweby [a], Sean Mayes [b,e], Erik H. Murchie [b], Asha S. Karunaratne [d], Festo Massawe [b,c], Marcus J. Tindall [a,f,*]

[a] Department of Mathematics and Statistics, University of Reading, Whiteknights, Reading, RG6 6AX, United Kingdom
[b] School of Biosciences, University of Nottingham, Sutton Bonington Campus, Loughborough, LE12 5RD, United Kingdom
[c] School of Biosciences, University of Nottingham Malaysia, Jalan Broga, 43500 Semenyih, Selangor Darul Ehsan, Malaysia
[d] Sabaragamuwa University of Sri Lanka, P.O. Box 02, Belihuloya, 70140, Sri Lanka
[e] Crops For the Future, Jalan Broga, 43500 Semenyih, Selangor Darul Ehsan, Malaysia
[f] Institute of Cardiovascular and Metabolic Research, University of Reading, Whiteknights, Reading, RG6 6AA, United Kingdom

ARTICLE INFO

Keywords:
Nonlinear ordinary differential equations
Coupled systems
Underutilised crops
Multiscale modelling

ABSTRACT

A principal objective in agriculture is to maximise food production; this is particularly relevant with the added demands of an ever increasing population, coupled with the unpredictability that climate change brings. Further improvements in productivity can only be achieved with an increased understanding of plant and crop processes. In this respect, mathematical modelling of plants and crops plays an important role. In this paper we present a two-scale mathematical model of crop yield that accounts for plant growth and canopy interactions. A system of nonlinear ordinary differential equations (ODEs) is formulated to describe the growth of each individual plant, where equations are coupled via a term that describes plant competition via canopy–canopy interactions. A crop of greenhouse plants is then modelled via an agent based modelling approach in which the growth of each plant is described via our system of ODEs. The model is formulated for the African drought tolerant legume bambara groundnut (*Vigna subterranea*), which is currently being investigated as a food source in light of climate change and food insecurity challenges. Our model allows us to account for plant diversity and also investigate the effect of individual plant traits (e.g. plant canopy size and planting distance) on the yield of the overall crop. Informed with greenhouse data, model results show that plant positioning relative to other plants has a large impact on individual plant yield. Variation in physiological plant traits from genetic diversity and the environmental effects lead to experimentally observed variations in crop yield. These traits include plant height, plant carrying capacity, leaf accumulation rate and canopy spread. Of these traits plant height and ground cover growth rates are found to have the greatest impact on crop yield. We also consider a range of different planting arrangements (uniform grid, staggered grid, circular rings and random allocation) and find that the staggered grid leads to the greatest crop yield (6% more compared to uniform grid). Whilst formulated specifically for bambara groundnut, the generic formulation of our model means that with changes to certain parameter's, it may be extended to other crop species that form a canopy.

1. Introduction

A changing climate and the ever increasing demands for food production in a growing world population require further improvements in agricultural productivity, which can only be achieved with an increased understanding of plant and crop processes. In this respect, mathematical modelling of plants and crops plays an important role. There has been a large amount of work undertaken in this area with two fundamental aims, firstly, to investigate and develop understanding of plant processes and secondly, to make predictions. The majority of this work, for either aim, focuses either on describing processes within a plant such as genetic regulatory networks (Hammer et al., 2002), descriptions of an entire plant in isolation (Yan et al., 2004) or the growth of many plants simultaneously, i.e. crop growth (Li et al., 2009).

Crop models provide a quantitative means of predicting growth, development and yield of a crop (Monteith et al., 1980). They are useful in modelling the interactions between crop growth and environmental

* Corresponding author at: Department of Mathematics and Statistics, University of Reading, Whiteknights, Reading, RG6 6AX, United Kingdom.
E-mail address: m.tindall@reading.ac.uk (M.J. Tindall).

https://doi.org/10.1016/j.jtbi.2022.111373
Received 1 April 2022; Received in revised form 22 November 2022; Accepted 24 November 2022
Available online 9 December 2022

factors; enabling an evaluation of growth limitation caused by climate factors (Aggarwal and Kalra, 1994). Even for one particular purpose there are many variations in the approaches used. Beyond crop models (those that deal with the aggregate plant scale), plant models (those that consider the single plant scale) are tools that can be used to better understand the underlying processes of crop development. The process of plant growth can be studied at several levels of detail, ranging from sub-plant to the multi-plant level.

At the crop scale, physiological processes at the plant scale are often taken for granted leaving biomass formation and food yield to be typically taken as a function of management factors, such as water irrigation and soil tillage (Goudriaan and Van Laar, 1994). It is a challenge in science to explain findings at the crop scale in terms of the physiological processes at the plant scale.

In this work we are concerned with understanding the effect that individual plant behaviour, in particular growth and plant–plant canopy interactions, has on the overall growth and development of the crop. We are interested in developing a mathematical framework that is computationally practicable and provides insight on the impact planting arrangements and genetic variability (between plants) has on the overall crop yield. Our mathematical model is constructed using the test crop of bambara groundnut (*Vigna subterranea*), an underutilised African legume which is currently being investigated for its ability to become a staple food crop in more arid areas of the world and in the context of a changing climate. Our mathematical model is developed in a way that it may be applied to other crop species, provided crop species form a plant canopy. Before detailing the physiological characteristics of bambara groundnut, we provide a brief overview of the mathematical modelling of individual plants to date.

Many models that work on the individual plant scale examine the allocation of assimilated nutrients for cell reproduction, hereby referred to as assimilates. Ma et al. (2010) discusses the growth of an individual plant in regards to its source–sink relationships, paying specific attention to competition between assimilates within the plant and plant topology, but do not discuss competition between plants. More examples of models of this nature can be found in Cieslak et al. (2011), Marcelis et al. (1998) and Zhang and DeAngelis (2020).

There has been an ever increasing importance placed on including plant architecture within models (Fourcaud et al., 2008). Godin Godin (1999) provides us with several methods of representing plant architecture with a range of complexities to be used in functional–structural models. More recently, Zhang and DeAngelis (2020) has reviewed Agent Based Models (ABMs) applied to the plant science, where both the individual and multi-plant level is considered. In both Godin (1999) and Zhang and DeAngelis (2020), complexity of the plant architecture ranges from coarse level representations such as modelling an entire plant structure as a single module to much finer levels where a tree's structure is split into many repeated components (e.g. branches, stems and leaves). At the most basic level, geometric representations of tree crowns can be used efficiently to model light interception. These geometric representations can take the form of a cylinder or sphere, but can also take more flexible and complex representations that come at an 'intermediate' computational cost between simpler geometric shapes and more elaborate computational representations. Models that investigate the more precise aspects of canopy structure are useful in examining processes such as the optimisation of photosynthesis. The application of these detailed architectural models to predicting whole crop yield is less obvious but it is clear such architectural features are important (Burgess et al., 2015). Limitations of these models include a limit to the number of possible individuals within the model. Additionally, the spatial locations of individuals relative to neighbours are not taken into account. Instead, shadowing is expressed as a function of available light.

In the cases where all plants within the crop are *not* treated as a single entity, an individual-based approach is used where the growth of each plant is described. Bauer et al. (2002) discusses the importance of including spatial positioning and a zone of influence where interactions with neighbours occur in individual-based methods. The aim of this work was to investigate the cyclic dynamics in perennial plant populations. The growth rate of individual plant size is determined using non-linear mathematical functions. In addition to the growth of individual plants, Bauer et al. model the change in population of a field of plants. Here, plant reproduction rate is determined by a linear relationship between individual plant size and the spatial positioning of newly introduced plants, using a two-dimensional exponential probability function. Plant mortality is determined by plant age and the degree of competition so that once the combined effect of these two variables meets a certain threshold, the plant is assumed to die.

The zone of influence model described by Cournede et al. (2008) is another individual-based model that describes crop scale growth. The zone of influence take the shape of a circle and is the area a single plant impacts upon. The growth of individual plants and the interactions between them is aggregated to the many plant level. The growth of a population of plants is simulated by coupling individual plants using the neighbour–neighbour competition for light. Here, competition is calculated as a function of spatial overlap between two plant canopies. Plant shadowing is calculated using a Poisson probability model that determines whether an infinitesimally small element of a plant's surface area is shadowed by a neighbouring plant. The model assumes strictly vertical irradiance and canopy foliage is uniformly distributed amongst the zone of influence. Despite these generalisations, the method gives a good general approach and applications of this methodology are far reaching.

In contrast to the generalised approach of Cournede et al. (2008) and Godin and Caraglio (1997) describes a more detailed topological method. In this case the plant is divided into its individual components and interactions between these are modelled using tree-graph structures. The components can be divided into spatial or mechanical ones. These models can be allowed to vary in time, however the process of doing this is somewhat arbitrary and consists of piecing together separate 'snap-shots' of the plants' topological structure.

The way in which competition is included in an individual-based model can vary. Schneider et al. (2006) explores a number of methods of incorporating inter-plant competition, which are referred to as competition kernels. These kernels include, but were not limited to, spatial overlap between two circular canopies, where canopy area was taken to be a function of biomass. The inter-plant competition for all kernels is limited to pairs of plants and does not explore the case of multiple plants overlapping at the same point. The interactions that one plant has with others is summed over all neighbouring plants. It was found in this work that zone of influence models were significantly more efficient at capturing crop behaviour and that there exists a large amount of asymmetry in competition, whereby if one of the two competing plants is significantly larger than the other, the smaller plant experiences the majority of competition.

Gaudio et al. (2021) discusses the importance of combining modelling approaches in order to best represent within and between plant process. In particular, the importance of recognising how traits that have been measured under fluctuating conditions are best characterised by functional models. For example, crop response to plant density and water-stress dynamics. In this same work, Gaudio et al. (2021) also provides examples where applying a simplified approach to modelling a certain process is appropriate. For example, applying the turbid-medium approach and Beer–Lambert law when modelling light partitioning among plants is sufficient and accuracy is only marginally improved by more complex models.

1.1. Bambara groundnut

Bambara groundnut is an underutilised crop species that has been recognised for its considerable ability to produce high yields in drought conditions (Aliyu et al., 2015). It is an annual herb that grows to

(a) (b)

Fig. 1. The bambara groundnut plant. Here (a) is a schematic of a typical plant canopy whilst (b) is a birds-eye view of a single plant 51 days after sowing.

approximately 30 cm high and is similar to the groundnut (peanut) in morphology in that it grows leaves on lateral stems just above ground level and develops pods containing seeds underground. Each pod contains between one and four seeds that are used for human and animal consumption. It can be categorised into three types; bunched, semi-bunched and spreading with the internode length determining which category it lies in. Seeds are variable in their shape, colour and hardness and it is the appearance of the pods along with the plants spreading type which determine which cultivar (plant variety) they belong to Linnemann and Azam-Ali (1993).

As an underutilised crop, there has been no rigorous breeding programmes as often occurs for established varieties (Aliyu et al., 2015). Instead it is landraces, defined as a locally adapted variety of a species, that are grown by farmers (Karunaratne, 2009). In this work, two such landraces are investigated namely, Uniswa Red and S19-3. Of these, S19-3 is considered to have been evolved for hot, dry climates causing it to have a faster life cycle, which minimises the potential damage caused by droughts. Uniswa Red is more adapted to wetter, colder climates and has a longer life cycle. For both landraces, germination occurs generally between seven and fifteen days depending on water availability, temperature and genetic variety (Cornelissen, 2005; Mwale et al., 2007). Plants begin to produce flowers between 30–55 days after sowing and fertilised flowers produce pods underground approximately 30 days after fertilisation (Linnemann and Azam-Ali, 1993). It has been found that the time from sowing to flowering is not always affected by the number of daylight hours in a day, however the time to podding is Azam-Ali et al. (2001). Leaves grow on multiple lateral stems that spread along the ground, as illustrated in Fig. 1.

There has been much work done in quantifying external (e.g. weather) and crop management effects on the yield of bambara groundnut (Alshareef, 2010; Mabhaudhi and Modi, 2013), but to date there has been little mathematical modelling of bambara as a crop. Work has not examined in detail the effect of canopy interactions on biomass production. Instead the total number of crops is treated as a single entity and competition is incorporated using a density factor (Cornelissen, 2005; Karunaratne et al., 2011). Current bambara groundnut mathematical models show reasonable similarities between simulations and experimental data, however these simulations are often site specific and underestimate above ground dry matter production in the greenhouse. It is theorised that this could be due to underestimating the photosynthetic potential of the plant (Cornelissen, 2005).

Karunaratne et al. (2011) discusses the importance of temperature in modelling bambara groundnut. Like many of the major crops such as wheat, cowpea and rice, bambara groundnut has been shown to be strongly affected by extremes in temperature. The BAMGRO model (Karunaratne, 2009) uses a system of dynamical deterministic equations to simulate the leaf development, plant biomass and pod mass of the entire crop. It operates between two interconnected processes: the progress through developmental phases and the rate of biomass acquisition. This work pays particular attention to the effect that temperature and drought have on growth at the crop level. Brink et al. (1999) recognises the strong link between photo-period and temperature on phenological development but applies it in a different way. Here a relatively simple method is applied to modelling bambara groundnut. The rate of progress towards a phenological stage is calculated using a combination of three linear equations that depend on temperature and photo-period. A benefit of this method is that the interaction of photoperiod and temperature on the influence on the crop disappears. This is beneficial as Brink et al. (1999) demonstrates that not all of the plants are affected by long photo-periods. The method has been applied to several types of annual crops such as soya bean, cowpea, chickpea, lentil and barley in the work of Summerfield et al. (1991).

In this paper we formulate, parameterise and analyse a multi-scale mathematical model describing the growth of bambara groundnut plants from the individual to many plant (crop) scale. The growth and development of each individual plant, which is assumed to consist of an individual stem and canopy, is described using the theory of nonlinear ordinary differential equations (ODEs). The individual plant model is parameterised using greenhouse data, analysed mathematically and model simulations compared with experimental data. A crop scale model is then generated by considering planted arrays of individual plants, whereby the growth and development of each plant is described by our governing system of ODEs. Interactions between plants occur via their canopies. The effect of canopy–canopy interactions is investigated in the context of the yield of individual plants as well as that of the overall crop. Our manuscript is organised as follows. In Section 2 we present our individual plant model. This is extended in Section 3 to the crop scale where we describe how canopy–canopy interactions between

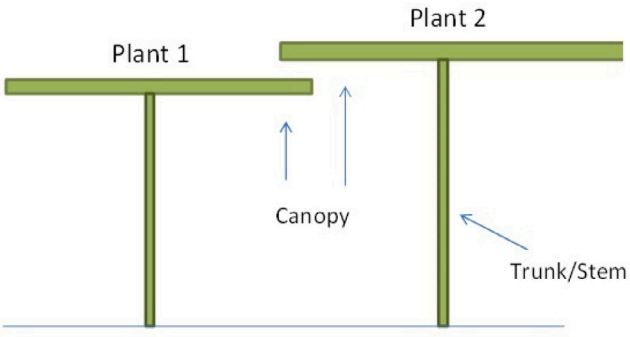

Fig. 2. Two competing plants, whose primary canopies we consider in this work comprises those parts of the canopy which receive direct sunlight. We assume each plant consists of a single stem and canopy. In this scenario Plant 2 has grown higher than Plant 1 thus overshadowing part of its canopy.

a plant and its neighbours are calculated, introduce our agent based algorithm and non-dimensionalise our governing ODEs. Steady-states of the individual plant model are analysed in Section 4 and model parameterisation discussed in Section 5. Numerical simulations of the crop scale model are presented in Section 6 and compared with experimental data. The model is numerically investigated further in Section 7, where key mechanisms responsible for affecting crop yield are identified via a sensitivity analysis, and how different planting layouts impact overall crop yield is considered in Section 7.2. Section 7.3 extends this analysis to consider the effect genetic variation between plants has on total yield. Our paper closes with a discussion and summary of our main findings in Section 8.

2. Individual plant model

For the purposes of this model, the plant canopy is simplified to a disc representing the upper most layer of leaves, raised above the ground by a core stem as shown in Fig. 2. This simplification assumes that the areas of the canopy that gain energy from direct sunlight are those that contribute most significantly to plant growth and development. It is likewise a restriction of sunlight to these areas of the canopy, via interaction with other plant canopies that diminishes the energy received. This approximation also simplifies the mathematical model allowing us to capture the effects of interplant competition without being computationally burdensome on the many plant scale. In addition, this simplified plant geometry is transferable to many other plants.

Like BAMGRO (Karunaratne et al., 2011), our model incorporates two interconnected processes: the crop maturation rate and the rate of biomass acquisition. Crop maturation rate, or crop phenology, are the different developmental phases of crop growth. Movement through these phases is considered non-reversible and strongly dependent on temperature. The developmental stages consist of two main phases, namely vegetative and reproductive. Unlike many grains used for food, where the change between vegetative and reproductive acts like a switch, these phases overlap for bambara groundnut. Thus the plant continues to develop new leaves in the reproductive stage.

The rate of leaf appearance is measured as a function of cumulative thermal time where thermal time is the sum of the average daily temperature above the critical value (Cornelissen, 2005; Karunaratne et al., 2011). This can be done in a number of ways, either the leaves per cumulative thermal time can be measured as a series of piecewise linear relationships (Cornelissen, 2005) or a Gaussian relationship can be used to model the new leaf rate (Karunaratne et al., 2011). This Gaussian approach has also been used in mathematical models of other plant species (Esnal and Lopez-Fernandez, 2010). The advancement in developmental (phenological) age, i.e. the stages of growth, is also measured in terms of thermal time. This is one of the most widely used approaches in crop models (Alm et al., 1988; Granier et al., 2002; Gramig and Stoltenberg, 2007; Karunaratne et al., 2011). It has been shown that phenological stages such as emergence, leaf initiation and leaf appearance rate occur at a precise thermal time after germination (Granier et al., 2002). In the BAMGRO model (Karunaratne et al., 2011), the leaf appearance rate and hence the leaf number and leaf area are calculated as a function of thermal time. This is then incorporated into the biomass acquisition equation to simulate the green biomass and crop yield. The method has been adopted in this work and the process is described in more detail in Section 2.2.

In what follows we describe the formulation of our mathematical model for one plant which includes a description of plant height, leaf area, ground cover, canopy and pod growth.

2.1. Plant height

The height of each plant is assumed to grow logistically and decay exponentially so that

$$\frac{dh(t)}{dt} = \alpha_h h(t)\left(1 - \frac{h(t)}{k_h}\right) - d_h h(t), \tag{1}$$

where α_h is the growth rate, k_h is the maximum height and d_h is the height decay rate.

2.2. Leaf area

To describe the growth in total leaf area over time, we first introduce a concept known as cumulative thermal time. Consider a critical temperature T_{crit} above which the plant will grow and below which it will not. The daily effective temperature $T_{eff}(T_{avg}, t)$ is then the average difference between the temperature and critical temperature over the day, subject to the temperature being greater than the critical temperature and below a maximum temperature T_{ceil}. For convenience, a piecewise linear function for temperature is applied, whereby samples taken each hour are assumed to describe the behaviour over the day. We then have

$$T_{eff}(T_{avg}, t) = \frac{1}{24}\sum_{j=1}^{24}\left(T_j(t) - T_{crit}\right), \tag{2}$$

where $T_j(t)$ is the sampled hourly temperature in one day, T_{crit} is the critical temperature required for growth, and j refers to the hour of the day. The average hourly temperature is given by $T_{avg}(t) = \sum T_j(t)/24$, which for convenience will be treated as constant for each day, but may change between days. By doing so, $T_{avg}(t)$ becomes the daily average temperature. Cumulative thermal time $T_C(T_{avg}, t)$ is the daily effective temperature integrated over a given period of time so that

$$T_C(T, t) = \int_0^{\mathrm{DAS}} T_{eff}(T, t)dt,$$

where DAS are the number of days after sowing. This concept is sometimes referred to as the thermal time or temperature sum (Karunaratne, 2009). The cumulative thermal time can be thought of as the number of temperature units that are required for plant growth and is measured in units known as 'degree days', thus the daily effective temperature is measured in 'degree days per day'.

During the vegetative phase, the rate of leaf development for bambara groundnut differs over time for different temperatures. However, when measured in degree days leaf production is constant for all temperatures (Karunaratne, 2009). When bambara groundnut passes from the vegetative to flowering and podding stages, leaf production continues but decreases significantly (Mkandawire, 2007).

Literature data indicates that leaf accumulation exhibits Gaussian like behaviour in relation to cumulative thermal time (Karunaratne, 2009), with a maximum growth rate $a_L(t)$, a time of peak growth $b_L(t)$,

and a time window where significant leaf growth occurs $c_L(t)$. Thus leaf area $A(t)$ growth rate can be described by

$$\text{Leaf area growth rate} = L_A a_L(T_{avg},t) exp\left(-\left(\frac{T_C(t)-b_L(T_{avg},t)}{c_L(T_{avg},t)}\right)^2\right), \tag{3}$$

where L_A is the leaf area per leaf and $a_L(T_{avg},t)$, $b_L(T_{avg},t)$, and $c_L(T_{avg},t)$ are all species specific parameters that depend on the daily effective temperature $T_{eff}(T_{avg},t)$. Here we assume for simplicity that $a_L(T_{avg},t) = aT_{eff}(T_{avg},t)$, $b_L(T_{avg},t) = bT_{eff}(T_{avg},t)$ and $c_L(T_{avg},t) = cT_{eff}(T_{avg},t)$, where a, b and c are positive constants.

Once the plant shifts from the vegetative stage to the flowering and podding phases, the primary sink in energy is no longer leaf development but is instead pod development. When this occurs, and to what degree, is subject to various stresses on the plant, the most critical of which is temperature. For high temperatures, pod growth is decreased, but leaf mass continues to increase, meaning that although the plant is producing pods, leaf production continues at a higher rate compared to lower temperatures. We account for this in our model by defining a temperature dependent degradation rate that decreases for high temperatures causing more biomass to be partitioned to the leaves. Thus, when the temperature is high the majority of absorbed energy is partitioned to leaf maintenance. Leaf degradation is thus described by

$$\text{Leaf area degradation rate} = d_l T_{sl}(T_{avg},t)A(t), \tag{4}$$

where d_l is a degradation rate constant and

$$T_{sl}(T,t) = \frac{T_{opt}-T_{crit}}{T_{avg}(t)-T_{crit}}. \tag{5}$$

Thus if the temperature is below the optimum growth value of T_{opt}, leaf area degradation increases and for temperatures above optimum leaf area degradation decreases. The further temperature deviates from the optimum, the further $T_{sl}(T_{avg},t)$ is from 1. Similarly to the daily effective temperature, a piecewise function can be used to model the temperature over time, making use of sampled or predicted data. It is not necessary that the sampled temperature points be equal to that used for the daily thermal temperature.

Bringing all this together, the rate of change of leaf area per plant $A(t)$ over time is given by

$$\frac{dA(t)}{dt} = L_A a_L(T_{avg},t)\exp\left(-\left(\frac{T_C(t)-b_L(T_{avg},t)}{c_L(T_{avg},t)}\right)^2\right) - d_l T_{sl}(T_{avg},t)A(t), \tag{6}$$

where $T_{sl}(T_{avg})$ is given by Eq. (5).

The data used to formulate this work has been collected from greenhouse experiments where temperature has been kept constant. As such, Eq. (2) need no longer be dependent on time at all and becomes

$$T_{eff}(T) = T_{avg} - T_{crit}, \tag{7}$$

where T_{avg} is the imposed average daily temperature. Note, the temperature is constant over time but different between experiments.

Cumulative thermal time can then be described by

$$T_C(T,t) = t \times T_{eff}(T). \tag{8}$$

Substituting Eqs. (7) and (8) into Eq. (6) gives

$$\frac{dA(t)}{dt} = L_A a T_{eff}(T)\exp\left(-\left(\frac{t-b}{c}\right)^2\right) - d_l T_{sl}(T)A(t). \tag{9}$$

Hereafter, temperature will be assumed constant and the impact of temperature changing with time will not be considered.

2.3. Ground cover

Whilst we have calculated the total leaf area of our canopy, not all of this area will be affected directly by light. In order to approximate how much of the canopy is intercepted by light radiation, we first need to calculate the canopy shadowing or ground cover the plant exhibits. Data was not available for the size of individual canopies and so as part of the development of this project, we conducted a study measuring canopy size over time for two different planting densities. The details and respective data of this study are described in Section 5. It was found that a Gaussian relationship similar to that devised for leaf area best describes the evolution of ground cover. This relationship allows us to determine when peak growth of the ground cover occurs, how wide the window of peak growth is and the maximum growth rate. We assume the maximum growth rate of the ground cover $G(t)$ will be a function of leaf area such that

$$\frac{dG(t)}{dt} = \alpha_g A(t)\exp\left(-\left(\frac{t-b_g}{c_g}\right)^2\right), \tag{10}$$

where α_g is the ground cover growth rate, b_g determines the time of peak growth and c_g determines the range of time for which peak growth occurs.

2.4. Canopy growth

Now that leaf area and ground cover have been determined, the growth rate of the canopy can be calculated. The intercepted radiation a plant canopy is able to absorb $R = R(t)$ through a canopy decreases exponentially in terms of intensity from those areas closest to sunlight. A well-established approximation for a plant's radiation absorption is given by the Beer–Lambert law (de Wit, 1965)

$$R(t) = R_0(1-\exp(-\kappa\gamma(t))). \tag{11}$$

Here R_0 is the available photosynthetically active radiation above the canopy, $\gamma(t)$ denotes the leaf area index, which is the leaf area per unit ground surface area and κ is the extinction coefficient. The extinction coefficient is determined by the leaf orientation and the angle of the light source with respect to the leaves, so it would be 1 for horizontal flat leaves with light incident from directly overhead; for other light directions, the extinction coefficient will no longer be 1 for such leaves. This method of calculating the absorbed radiation is common in plant models and typically $\gamma(t)$ is calculated so that the total leaf area of all plants is divided by the total plot area. In this case, we are considering a single plant and hence we adapt the local area index such that it is defined as the ratio between plant leaf area and ground area per plant

$$\gamma(t) = \frac{A(t)}{G(t)}, \tag{12}$$

where $A(t)$ is the total leaf area of the canopy (given by the solution of Eq. (3)) and $G(t)$ is the ground cover of the plant's canopy (given by the solution of Eq. (10)) (Cournede et al., 2008). Here, $\gamma(t)$ can be thought of as the thickness of the disc that represents a plant canopy; $\gamma(t) > 1$ would imply that the leaf area is greater than the ground cover with multiple layers of leaves and thus a thicker disc. Conversely, $\gamma(t) < 1$ implies that the leaf area is less than the ground cover area which would indicating spread out leaves in a single layer.

To find the total radiation that has been absorbed by a plant, the total radiation per area $R(t)$, given by Eq. (11), needs to be multiplied by the surface area of the plant's canopy which intercepts the radiation i.e. the ground cover $G(t)$. After absorbing the photosynthetically active radiation, the plant must then convert that energy into biomass. This is incorporated into the model by including an efficiency coefficient c_e, which describes the mass gained per unit of radiation. In addition, no matter how much radiation the plant is exposed to, there is a maximum size the plant can reach. This limiting factor is incorporated via the

inclusion of a carrying capacity k_c, so that as biomass approaches k_c, the growth rate decreases.

Combining the total incoming radiation with the plant's ability to convert radiation into mass gives the canopy biomass ($c(t)$) growth rate

$$\text{Canopy growth rate} = c_e R(t) G(t) \left(1 - \frac{c(t)}{k_c}\right). \tag{13}$$

There is also some amount of canopy decay due to leaf senescence and pests. This is assumed proportional to the size of the canopy and is given by

$$\text{Canopy decay rate} = d_c c(t), \tag{14}$$

where d_c is the biomass decay rate and is assumed constant. By combining the relationships described in Eqs. (13) and (14) the change in canopy biomass over time can be written as

$$\frac{dc(t)}{dt} = c_e R_0 G(t) \left(1 - e^{-\kappa\gamma(t)}\right) \left(1 - \frac{c(t)}{k_c}\right) - d_c c(t), \tag{15}$$

where $R(t)$ has been substituted for as given by Eq. (11).

2.5. Pod growth

We derive an equation describing pod growth on an individual plant. Using pod mass experimental data for S19-3 and Uniswa Red (Karunaratne, 2009) the time at which podding commences can be extracted. It was found that for all three temperatures 63 and 75 days were indicative of pod initiation for S19-3 and Uniswa Red, respectively.

It is assumed here that the increase in pod mass $P(t)$ is a proportion of the increase in canopy biomass $c(t)$. Hence the growth rate of $P(t)$ is a function of the growth rate of $c(t)$. We further assume that as pod mass increases it becomes a stronger sink for absorbed energy and hence acquires a larger proportion of canopy biomass growth as it itself becomes larger. Thus, the change in $P(t)$ in time depends on both the rate of canopy biomass growth and the mass of the pod itself. We finally assume that pod mass cannot be larger than the canopy biomass and so $c(t)$ is the carrying capacity for pod mass. Thus the change in pod mass over time is given by

$$\frac{dP(t)}{dt} = \alpha_P T_{sp}(T) \frac{dc(t)}{dt} P(t) \left(1 - \frac{P(t)}{c(t)}\right) - d_p P(t), \tag{16}$$

where α_p is a growth rate for pod mass, $T_{sp}(T)$ is a temperature stress and d_p is the pod decay rate.

The temperature stress is only in effect for high temperatures and is a parameter that ranges between 0 and 1, where 1 indicates no stress. Hence T_{sp} is given by

$$T_{sp}(T_{avg}) = \begin{cases} 1, & T_{avg} \le T_{opt}, \\ 1 - \left|1 - \omega \frac{T_{avg} - T_{crit}}{T_{opt} - T_{crit}}\right| & T_{opt} < T_{avg} < T_{ceil}, \\ 0 & T_{avg} \ge T_{ceil}, \end{cases} \tag{17}$$

where ω is a species specific parameter to be determined and controls how far temperature stress decreases from 1 as temperature increases from the optimum.

2.6. Single plant model summary

To summarise, the system of equations that simulate the growth of a single plant is described by

$$\frac{dh(t)}{dt} = \alpha_h h(t) \left(1 - \frac{h(t)}{k_h}\right) - d_h h(t), \tag{18}$$

$$\frac{dT_C(t)}{dt} = T_{eff}(T_{avg}), \tag{19}$$

$$\frac{dA(t)}{dt} = L_A a T_{eff}(T_{avg}) \exp\left(-\left(\frac{t-b}{c}\right)^2\right) - d_l T_{sl}(T_{avg}) A(t), \tag{20}$$

$$\frac{dG(t)}{dt} = \alpha_g A(t) \exp\left(-\left(\frac{t-b_g}{c_g}\right)^2\right), \tag{21}$$

$$\frac{dc(t)}{dt} = c_e R_0 G(t) \left(1 - e^{-\kappa\gamma(t)}\right) \left(1 - \frac{c(t)}{k_c}\right) - d_c c(t), \tag{22}$$

$$\frac{dP(t)}{dt} = \alpha_P T_{sp} \frac{dc(t)}{dt} P(t) \left(1 - \frac{P(t)}{c(t)}\right) - d_p P(t), \tag{23}$$

where

$$T_{eff}(T_{avg}) = T_{avg} - T_{crit}, \qquad T_{sl}(T_{avg}) = \frac{T_{opt} - T_{crit}}{T_{avg} - T_{crit}} \quad \text{and} \quad \gamma(t) = \frac{A(t)}{G(t)}, \tag{24}$$

with the initial conditions

$$T_C(0) = 14 T_D(0), \quad A(0) = L_A, \quad G(0) = L_A, \quad c(0) = c_0 \quad \text{and} \quad P(0) = 0.$$

These conditions assume the plant has emerged (around day 14 following germination for bambara groundnut), with the leaf area equivalent to one fully emerged leaf denoted L_A which leads to a canopy size of c_0, and pods have yet to form.

Eq. (18) decouples from the remaining equations and can be solved in closed form to yield

$$h(t) = \frac{h_0(\alpha_h - d_h)\exp((\alpha_h - d_h)t)}{\alpha_h - d_h - \alpha_h K_h h_0 + \alpha_h K_h \exp((\alpha_h - d_h)t) h_0} \tag{25}$$

where $K_h = 1/k_h$ Whilst plant height is somewhat superfluous in the context of modelling a single plant, it will become critical when considering the difference in height between two or more plants and thus the effect of intercanopy competition as discussed in Section 3.1.

3. Crop scale model

To scale from the single plant to many plant scale, we need to consider competition between the plants for resources. It was stated in Section 2 that plant canopies are assumed to be circular discs raised above the ground by a central stem. The disc represents the layers of leaves within the canopy which are directly affected by sunlight. Similarly, it has been stated that light and temperature are the only limiting growth factors. Since temperature is not a competitive resource, the only form of competition we are interested in is that for light as a result of canopy–canopy shadowing. A plant that shadows another plant blocks sunlight from reaching the shorter plant's canopy so that competition for sunlight between plants will depend on which plant is taller. The inter-plant competition can then be described by the proportion of the lower canopy that is shadowed by the taller one. In order to account for the effect of canopy–canopy interactions on plant growth we proceed as follows.

3.1. Inter-plant competition

Determining the proportion of dynamically varying canopy–canopy interactions can be challenging as the following example illustrates. Consider the case of three intersecting plant canopies illustrated in Fig. 3. The proportion of area that canopy 1 (c_1) shares with canopy 2 and 3 (c_2 and c_3), cannot be found by summing the intersection of canopies 1 and 2 (I_{12}) and the intersection of canopies 1 and 3 (I_{13}). Instead, it is necessary to find the area that all three canopies share (I_{123}). Finding this area analytically is challenging and thus a numerical method for calculating canopy overlap was devised. This method is described in what follows.

We consider the competition any canopy c_i experiences with neighbouring canopies denoted c_k. Let canopy i be filled with n uniformly allocated points, a distance d apart. Sampling points are arranged in a series of increasing rings within the canopy where d is the distance between rings and the distance between points within a ring. Each point, labelled with a j, is allocated an x and y coordinate denoted

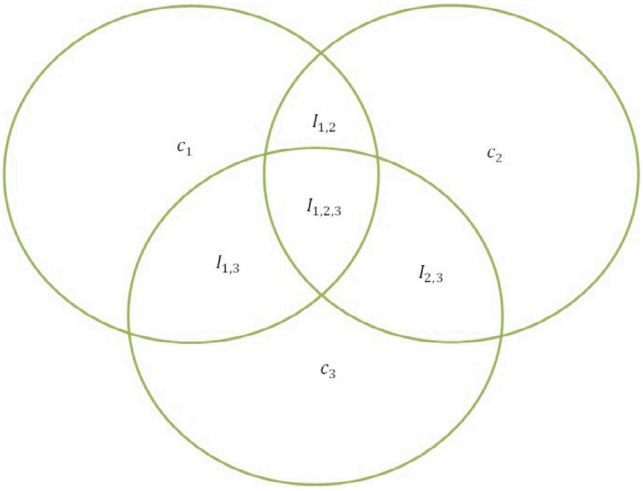

Fig. 3. Three intersecting canopies (c_1, c_2, c_3) that represent three neighbouring plants, where the areas of intersection are labelled as $I_{1,2}, I_{1,3}, I_{2,3}$ and $I_{1,2,3}$.

x_j and y_j, respectively. Each point within canopy i can now be tested to determine which canopies, other than canopy i, it lies within.

Let the centre point of canopy k have coordinates c_{kx} and c_{ky} and radius r_k. Then a sampling point within canopy i that is also within canopy k holds according to the condition that

$$\sqrt{(x_j - c_{kx})^2 + (y_j - c_{ky})^2} < r_k.$$

Then an $n \times N$ array A can be defined such that

$$A_{j,k} = \begin{cases} 1, & \text{if } \sqrt{(x_j - c_{kx})^2 + (y_j - c_{ky})^2} < r_k, \\ 0, & \text{otherwise,} \end{cases}$$

where N is the number of neighbouring circles and n is the number of sampling points within canopy i. An element $A_{j,k}$ equals 1 if sampling point j is within canopy k, but is otherwise zero. Summing the elements of each row of A gives a column vector B such that

$$B_j = \sum_{k=1}^{N} A_{j,k}.$$

Each element of vector B gives the number of circles that each sampling point j is contained in. All sampling points are contained within at least canopy i and so the minimum value of B_j is 1.

To find the proportion of area canopy i shares with neighbouring circles we must find the number of points that are contained within canopy i only, and so we define a $1 \times n$ vector C such that

$$C_j = \begin{cases} 1, & \text{if } B_j = 1 \\ 0, & \text{otherwise.} \end{cases} \tag{26}$$

Then the proportion of canopy i that is shared with adjacent canopies j is given by

$$O_i = 1 - \frac{\sum_{j=1}^{n}(C_j)}{n}. \tag{27}$$

The arrays A, B and C are calculated for each circle in turn to find O_i, $i \in [1, N]$. Hence $\mathbf{O}$ will be a vector of length N.

Clearly the accuracy of the numerical method depends on the number of sampling points n contained within the given canopy. It was found that there was little improvement between 5000 and 10 000 sampling points, however using 10 000 sampling points instead of 5000 increases computational time by approximately 24%. When calculating the area of intersection for many plants at multiple time points, the increase to computational time will add up considerably and so using 5000 sampling points is preferable. The error decreases for larger intersection areas but there is no obvious change in error for increased circle sizes. There was no obvious bias for the method to underestimate or overestimate the area of intersection. From this investigation we conclude 5000 sampling points will give a good approximation of $\mathbf{O}$.

We now consider how this method transfers to measuring the amount of shadowing between plant canopies. Plant canopies are represented using circular discs, however in the method devised for calculating overlap described in this section the intersection area has only been considered in a 2-D space. By doing this we have neglected to consider the heights of the plants. The area we wish to calculate is the proportion of plant canopy that is being shadowed by its neighbours and to do this, the plant height plays a key role in the calculation. To account for this we define an $N \times 1$ vector such that

$$\omega_{1k} = H_1(h_k - h_i),$$

where h_i is the height of Plant i, h_k is the height of a neighbouring Plant k and H_1 is a Heaviside function such that

$$H_1(x) = \begin{cases} 1, & \text{if } x > 0, \\ 0, & \text{otherwise.} \end{cases}$$

Thus

$$\omega_{1k} = \begin{cases} 1, & \text{if Plant } k \text{ is taller than Plant } i, \\ 0, & \text{otherwise.} \end{cases}$$

Let P_1 be an $N \times 1$ vector such that

$$P_{1j} = \sum_{k=1}^{N} A_{j,k}\omega_{1k},$$

then P_1 will give a list of the sampling points that are overlapped by plants that are strictly taller than Plant i. If $SUM(P_1) > 1$ then several plants overlap point j. Since we are not currently considering the case of light penetrating the canopy we do not need to concern ourselves with how many plants overlap point j only that some do. Therefore we let

$$C_{2j} = \begin{cases} 1, & \text{if } P_{1j} = 0, \\ 0, & \text{otherwise.} \end{cases} \tag{28}$$

The proportion of area that plant i shares with taller plants can then be found as

$$OT_i = 1 - \frac{\sum_{j=1}^{n}(C_{2j})}{n}. \tag{29}$$

For plants of the same height we assume that the leaves of the plant canopies intermingle and that overlap is distributed evenly over the competing canopies. Hence we assume each canopy receives half the amount of shadowing within the area of intersection. We define ω_2 such that

$$\omega_{2k} = H_2(h_k - h_i),$$

where H_2 is a Heaviside function defined such that

$$H_2(x) = \begin{cases} 0.5, & \text{if } x = 0, \\ 0, & \text{otherwise.} \end{cases}$$

Thus

$$\omega_{2k} = \begin{cases} 0.5, & \text{if Plant } k \text{ is the same height as Plant } i \\ 0 & \text{otherwise.} \end{cases}$$

A value of $\omega_{2k} = 0.5$ indicates that Plant i is competing with a plant of the same height and so the competition is split evenly between both plants. The case of $\omega_{2k} = 0$ refers to any other scenario. Now let P_2 be an $N \times 1$ vector such that

$$P_{2j} = \sum_{k=1}^{N} A_{j,k}\omega_{2k}.$$

The minimum value that an element of P_2 can take is 0.5 as each point is at least contained within canopy i, which is the same height as itself. When $P_{2j} > 1$ the point j is sharing the space with more than 1 other plant. Since competition is shared evenly among plants in the same spatial location we must take into account the number of plants point j is contained within. Then the proportion of Plant i shared with plants of the same height is

$$OS_i = 1 - \frac{\sum_{j=1}^{n}\left(\frac{0.5}{P_{2j}}\right)}{n}. \tag{30}$$

The total proportion of plant canopy i that is shadowed is then the sum of that shadowed by taller plants and those of the same height such that

$$O_i = OT_i + OS_i. \tag{31}$$

The impact that canopy shadowing has on the growth of a single plant needs to be accounted for in Eqs. (18)–(23). It is applied by including a shadowing factor $(1 - O_i)$, where $O_i(h_1, h_2, \dots, h_N)$ is the proportion of an individual canopy that is shadowed. Shadowing affects different plant growth processes and it is thus included in several parts of the model.

The leaf area and canopy biomass growth rates are affected as accumulation is affected by reduced sunlight caused by competition. The combined effects of lack of space, competition for nutrients and lack of sunlight prevent the plant reaching its maximum size. Therefore, in addition to the growth rate a varying carrying capacity has been included so that the plant is unable to grow unencumbered into a space occupied by another plant. The true carrying capacity, k_{max}, remains constant.

The morphology of bambara groundnut is such that it grows leaves on lateral stems above ground. Thus when bambara groundnut plants start overlapping, their canopies begin to intertwine. This causes a physical obstacle for plants when spreading and hence the window of peak ground cover spreading is affected. This prevents a plant continuing to spread into a space occupied by another plant.

Due to the morphology of bambara groundnut, we assume that the plant reaches its full height very quickly and then spreads. We therefore have excluded competition effects on height. Differences in height between plants are a consequence of their carrying capacity and so a plant with the potential for a greater height, reaches this height before its neighbours. If the model was to be extended to crops of different species where this assumption does not hold, it would be necessary to include the effects of competition in the height equation also.

To summarise, in this model competition affects:

- the maximum leaf area growth rate;
- the maximum ground cover growth rate via the leaf area term;
- the window of peak ground cover spreading;
- the growth rate of canopy biomass; and
- the carrying capacity of canopy biomass.

This also implies that overlap also affects the growth rate and carrying capacity of pod mass as these are functions of canopy biomass.

Eqs. (18)–(23) are thus revised to incorporate these effects for a crop of up to N plants, so that for any plant i

$$h_i(t) = \frac{h_{i0}(\alpha_h - d_h)\exp((\alpha_h - d_h)t)}{\alpha_h - d_h - \alpha_h K_{hi} h_{i0} + \alpha_h K_{hi}\exp((\alpha_h - d_h)t)h_{i0}}, \tag{32}$$

$$\frac{dT_{Ci}(t)}{dt} = T_{eff,i}(T_{avg}), \tag{33}$$

$$\frac{dA_i(t)}{dt} = L_A a_i T_{eff,i}(T_{avg})(1 - O_i(h_1, h_2, \dots, h_N))\exp\left(-\left(\frac{t - b_i}{c_i}\right)^2\right) - d_{Li} T_{sl,i}(T_{avg}) A_i(t), \tag{34}$$

$$\frac{dG_i(t)}{dt} = \alpha_{gi} A_i(t)\exp\left(-\left(\frac{t - b_{gi}}{c_{gi}(1 - O_i(h_1, h_2 \dots h_N))}\right)^2\right), \tag{35}$$

$$\frac{dc_i(t)}{dt} = c_{ei} R_0 G_i(t)\left(1 - e^{-\kappa\gamma_i(t)}\right)(1 - O_i(h_1, h_2, \dots, h_N)) \times \left(1 - \frac{c_i(t)}{k_{ci}(1 - O_i(h_1, h_2, \dots, h_N))}\right) - d_{ci} c_i(t), \tag{36}$$

$$\frac{dP_i(t)}{dt} = \alpha_{Pi} T_{sp} P_i(t)\frac{dc_i(t)}{dt}\left(1 - \frac{P_i(t)}{c_i(t)}\right) - d_{pi} P_i(t), \tag{37}$$

where

$$T_{eff,i}(T_{avg}) = T_{avg} - T_{i,crit}, \qquad T_{sl,i}(T_{avg}) = \frac{T_{opt} - T_{i,crit}}{T_{avg} - T_{i,crit}} \quad \text{and} \quad \gamma_i(t) = \frac{A_i(t)}{G_i(t)}, \tag{38}$$

with the initial conditions

$$T_{Ci}(0) = 14T_{eff}, \quad A_i(0) = L_A, \quad G_i(0) = L_A, \quad c_i(0) = c_0 \quad \text{and} \quad P_i(0) = 0, \tag{39}$$

and $O_i(h_1, h_2, \dots, h_N)$ is the overlap effect as a result of the canopy of plant i being affected by neighbouring plants of height $h_1, h_2 \dots h_N$.

3.2. Non-dimensionalisation

Eqs. (32) to (39) are non-dimensionalised according to the following rescaling's

$$h_i(t) = h_0\hat{h}_i(t), \quad T_{Ci}(t) = \frac{T_{eff}}{\alpha_h}\hat{T}_{Ci}(\tau), \quad c_i(t) = c_0\hat{c}_i(\tau),$$

$$G_i(t) = L_A\hat{G}_i(\tau), \quad A_i(t) = L_A\hat{A}_i(\tau), \quad P_i(t) = c_0\hat{P}_i(\tau), \quad \text{and} \quad t = \frac{\tau}{\alpha_h},$$

where a hat signifies a non-dimensional physical variable and τ denotes non-dimensional time. Then the non-dimensional system of equations is given by

$$\hat{h}_i(\tau) = \frac{h_0(1 - \bar{d}_h)\exp((1 - \bar{d}_h)\tau)}{1 - \bar{d}_h - K_{hi}h_0 + K_{hi}\exp((1 - \bar{d}_h)\tau)h_0}, \tag{40}$$

$$\frac{d\hat{T}_{Ci}(\tau)}{d\tau} = 1, \tag{41}$$

$$\frac{d\hat{A}_i(\tau)}{d\tau} = \bar{a}_{Li}\left(1 - O_i(\hat{h}_1, \hat{h}_2, \dots \hat{h}_N, \tau)\right)exp\left(-\left(\frac{\tau - \bar{b}_i}{\bar{c}_i}\right)^2\right) - \bar{d}_{Li}T_{sp}\hat{A}_i(\tau), \tag{42}$$

$$\frac{d\hat{G}_i(\tau)}{d\tau} = \bar{\alpha}_{gi}\hat{A}_i(\tau)exp\left(-\left(\frac{\tau - \bar{b}_{gi}}{\bar{c}_{gi}(1 - O_i(\hat{h}_1, \hat{h}_2, \dots \hat{h}_N, \tau))}\right)^2\right), \tag{43}$$

$$\frac{d\hat{c}_i(\tau)}{d\tau} = \bar{\alpha}_{ci}\left(1 - exp(-\kappa_i\hat{\gamma}_i(\tau))\right)\hat{G}_i(\tau)\left(1 - \bar{K}_{ci}(O_i, \tau)\hat{c}_i(\tau)\right) \times \left(1 - O_i(\hat{h}_1, \hat{h}_2, \dots \hat{h}_N, \tau)\right) - \bar{d}_{ci}\hat{c}_i(\tau), \tag{44}$$

$$\frac{d\hat{P}_i(\tau)}{d\tau} = \bar{\alpha}_{Pi}T_{sp}\hat{P}_i(\tau)\frac{d\hat{c}_i(\tau)}{d\tau}\left(1 - \frac{\hat{P}_i(\tau)}{\hat{c}_i(\tau)}\right) - \bar{d}_{pi}\hat{P}_i(\tau), \tag{45}$$

where

$$T_{sl,i}(T) = \frac{T_{opt} - T_{i,crit}}{T_{avg} - T_{i,crit}} \quad \text{and} \quad \hat{\gamma}(\tau) = \frac{\hat{A}(\tau)}{\hat{G}(\tau)}, \tag{46}$$

with the initial conditions

$$\hat{T}_{Ci}(0) = 14, \quad \hat{A}_i(0) = 1, \quad \hat{G}_i(0) = 1, \quad \hat{c}_i(0) = 1 \quad \text{and} \quad \hat{P}_i(0) = 0, \tag{47}$$

The non-dimensional parameters are stated in Table 3. Hereafter, hats and bars will be omitted for notational convenience.

3.3. Crop scale model algorithm

We now outline our algorithm for determining the growth and development of a crop of N plants, planted in a predefined spatial arrangement. To summarise our mathematical model comprises a system of 6 nonlinear equations per plant as given by Eqs. (32)–(39);

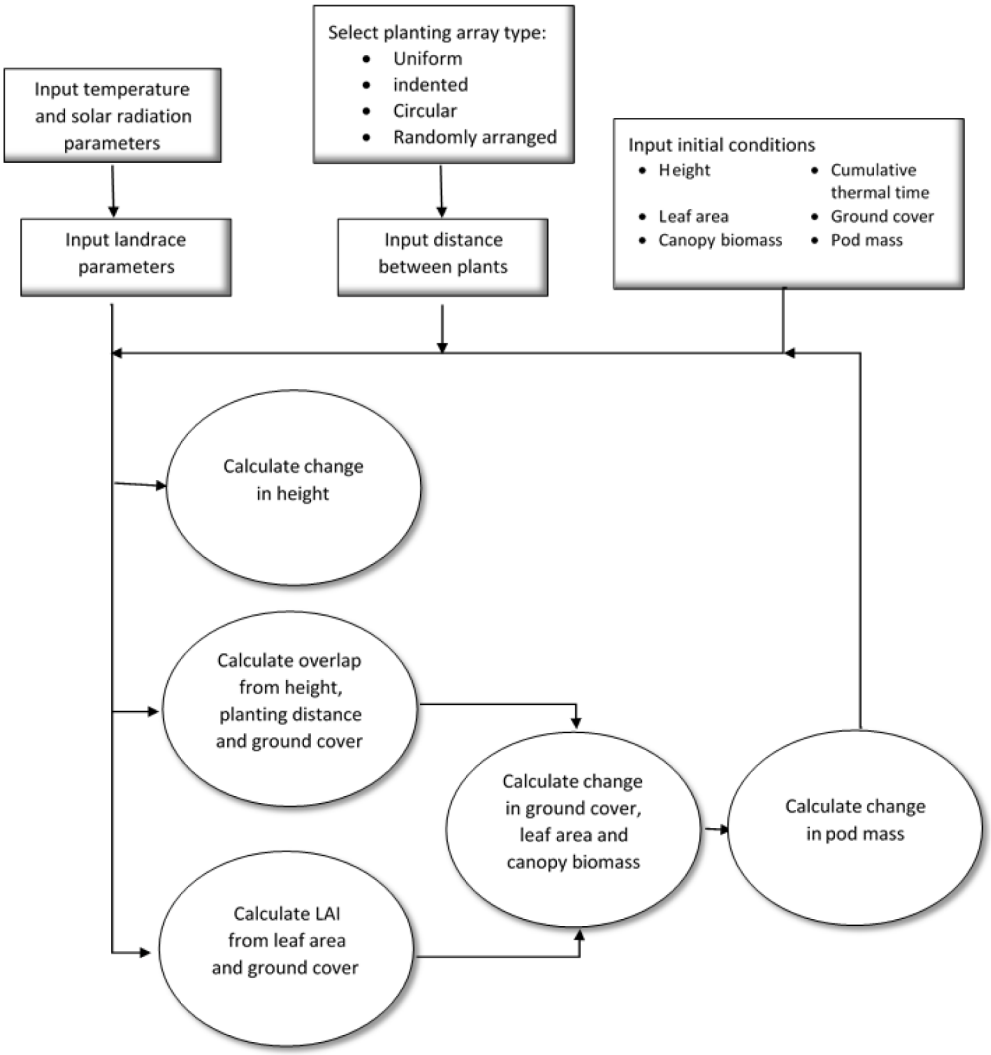

Fig. 4. A schematic overview of the key steps in the crop scale model algorithm.

one equation describing plant height and 5 ODEs detailing cumulative thermal time, leaf area, ground cover, canopy biomass and pod mass. This gives a total of $6 \times N$ equations per plant where N is the number of plants in a simulation.

In order to model a crop of N plants, we detail an algorithm where each plant is treated as an individual entity arranged on a two-dimensional spatial grid with varying layouts (uniform, indented, circular and random) as shown in Fig. 14, henceforth referred to as the planting layout. The competition between neighbouring plants is described by canopy–canopy shadowing where the respective heights of each plant determine the competition they experience.

The steps of our algorithm are summarised in Fig. 4 and are as follows.

1 Input parameters for the chosen landrace of bambara groundnut as described in Section 4.
2 Input temperature and solar radiation data R_0 as described in Section 4.
3 Choose planting layout (uniform grid, partially indented grid, circular pattern and random) illustrated in Fig. 14.
4 Input the distance between plants.
5 Enter the initial conditions describing height, thermal time, leaf area, ground cover, canopy biomass and pod mass per plant.
6 Calculate LAI from leaf area and ground cover.
7 Calculate plant height from Eq. (40).
8 Calculate the inter-plant competition experienced by each plant using its ground cover, height and position as detailed in Section 3.1.
9 Calculate the rates/derivatives for height, cumulative thermal time, leaf area, ground cover, canopy biomass and pod mass per plant defined by Eqs. (40) to (47).
10 Set $t = t + \delta t$ where δt is the internal time step chosen by the Matlab ODE solving algorithm ODE15s so that the absolute and relative error tolerances are met.
11 Repeat steps 3–7 until the plant reaches maturity [assumed to be 150 days after sowing for bambara groundnut] at $t = T_{end}$.

This algorithm was implemented in Matlab R2015b in Windows 10.

4. Steady-state analysis

It is difficult to obtain a closed form analytical solution to the system of Eqs. (41)–(47). However, we wish to check that the model exhibits bounded behaviour which is biologically consistent. One relatively straightforward check is to determine the system steady-states which we do so as follows.

We first observe that Eq. (42) is non-autonomous. As such, a steady-state would not exist as any solution to $\frac{dA_i(\tau)}{d\tau} = 0$ would depend on τ. Therefore, we need to examine the behaviour of $\frac{dA_i(\tau)}{d\tau}$ as $\tau \to \infty$. Doing

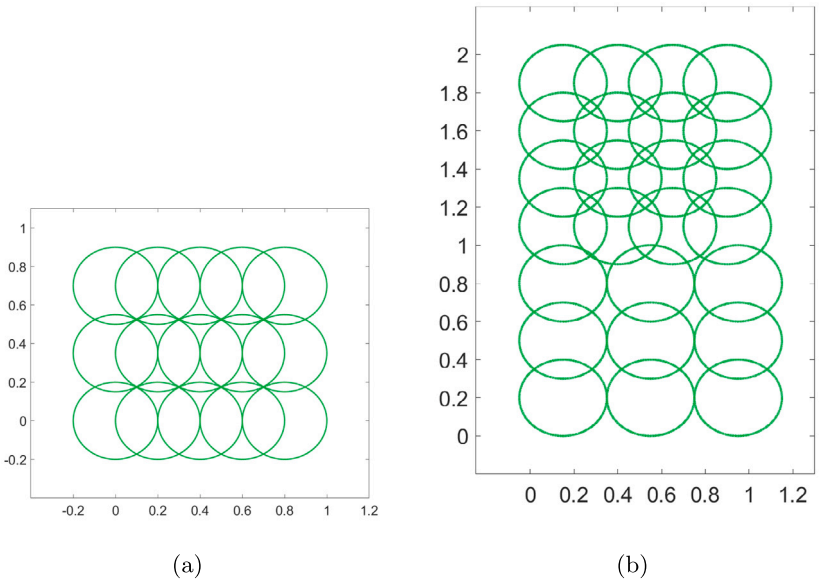

Fig. 5. Planting layout of the two experiments that have provided data used to parameterise the model. Here (a) is for the TCRU experimental data and (b) is for the FCG experiments.

so leads to

$$\lim_{\tau\to\infty}\frac{dA_i(\tau)}{d\tau} = \lim_{\tau\to\infty}(-\bar{d}_L A_i(\tau)),$$

and thus

$$\lim_{\tau\to\infty} A_i(\tau) = \lim_{\tau\to\infty} e^{-\bar{d}_L\tau} = 0,$$

providing $d_L > 0$, which it is by definition. From Eqs. (44) and (45) it can be seen that if $d_c > 0$ and $d_p > 0$ then $c_i \to 0$ and $P_i \to 0$ as $\tau \to \infty$, since the growth rate of $c_i(\tau)$ and therefore $P_i(\tau)$ depend on $A_i(\tau)$. Thus our asymptotic system of equations for N plants goes to

$$\lim_{\tau\to\infty} h(\tau) = \frac{(1-\bar{d}_h)}{K_{hi}}, \quad \lim_{\tau\to\infty} A(\tau) = 0, \quad \lim_{\tau\to\infty} G(\tau) = 0 \tag{48}$$

$$\lim_{\tau\to\infty} c(\tau) = 0 \quad \text{and} \quad \lim_{\tau\to\infty} P(\tau) = 0. \tag{49}$$

Clearly this is non-physical since it is impossible for a plant without any biomass to have an associated height. However, as the height is only of interest when comparing the heights of neighbouring plants, we are able to satisfy ourselves with the result. As an annual crop, bambara groundnut completes its life cycle. Thus, by tending to zero, the long term growth behaviour of leaf area and canopy biomass is being correctly captured by the model equations.

5. Model parameterisation

The model has been parameterised using a range of techniques including values sourced from the literature, informed estimates of unknown parameters and model-data fitting of experimental data. The values of all dimensional parameters are given in Table 2. Parameters values were determined as follows.

The parameters T_{opt}, T_{crit}, k_{max}, PAR, e and k_i have all been taken directly from the literature, the values and sources of which can be found in Table 2. Experimental data has shown that plant height reaches steady-state at a much faster rate when compared to leaf area, canopy biomass, ground cover and pod mass. The parameters α_h and d_h have been approximated using a 'best-guess' approach, to simulate this behaviour.

The remaining parameters, L_A, k_{max}, a, b, c, d_L, c_e, d_c, k_h, α_g, b_g and c_g have been informed using data collected from a series of greenhouse experiments. The first of the two sets of greenhouse experiments were conducted in the Tropical Crops Research Unit (TCRU) located in the Sutton Bonington campus of the University of Nottingham, UK (Karunaratne, 2009). This data consists of two species: Uniswa Red and S19-3, grown at temperatures of 23 °C, 28 °C, and 33 °C, respectively. Leaf number, leaf area, leaf mass, stem mass, root mass, pod mass and total biomass were monitored over sixteen day intervals starting at thirty three days post seed sowing. Data were collected using a destructive process and so details regarding the growth of one plant in isolation cannot be retained. Plants were planted with an initial distance of 35 cm between columns D_c and 10 cm between rows D_r, with plants being removed at germination so that the distance between rows became 20 cm. The supply of water was non-limiting. A more detailed description of the experimental methodology can be found in Karunaratne (2009). Shutters were applied onto the greenhouse to impose day lengths of no longer than 12 h. This is because previous experiments have found that longer day lengths affect phenological development and have a negative impact on yield.

The leaf area per leaf L_A and the carrying capacity for the canopy biomass k_{max} is extracted directly from the TCRU experimental data. The leaf area per leaf for one plant of N at one sampling time of J is given by the ratio between leaf area $A_{i,j}$ and leaf number $L_{i,j}$, where i indicates the plant and j the sampling time. The leaf area per leaf for this model L_A was found by averaging this ratio for all sampled plants such that

$$L_A = \frac{1}{NJ}\sum_{j=1}^{J}\sum_{i=1}^{N}\frac{A_{i,j}}{L_{i,j}}.$$

The carrying capacity has been taken to be the largest observed biomass in the experiment.

The values of a, b, c, d_L, c_e and d_c were further refined by taking least-squares fit of the TCRU experimental greenhouse data against a model simulation for a temperature of 28 °C. Since plant position is an important feature in this model framework, the positions of simulated plants have been set to match the arrangement in the experiments; the layouts for both experiments and the corresponding simulations is given in Fig. 5. The inbuilt MATLAB function lsqcurvefit, which is a non-linear least-squares solver, was then used to conduct the least-squares fit.

A second set of greenhouse experiments were conducted for this study at the Future Crops Greenhouses (FCG) located in the Sutton Bonnington campus of the University of Nottingham. The aim of these experiments was to provide data on individual plant size and the

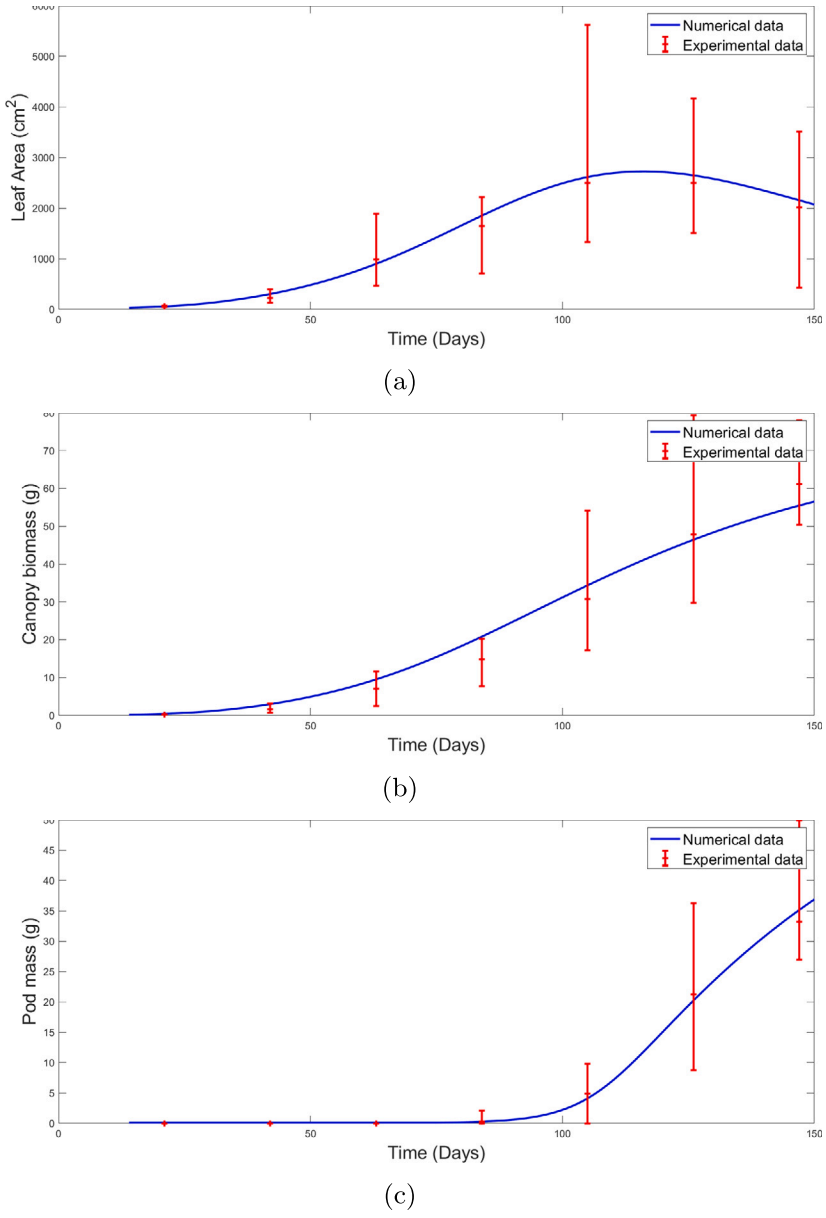

Fig. 6. The simulated (a) leaf area, (b) canopy biomass and (c) pod mass compared with the experimental data for the species Uniswa Red, using the data-fitted case of a temperature of 28 °C. Red bars indicate the upper and lower bounds of the experimental data.

magnitude of inter-canopy plant competition. This data allows us to inform and investigate how changes in planting density affect yield. All plants were transplanted 10 days after emergence and harvested after a further 132 days. The collected data comprised the diameter of the plant canopy measured at the widest point every two weeks, the dry canopy biomass per plant at harvest and the dry pod mass per plant at harvest. On harvest the number of pods per plant were recorded and separated from the remaining above ground biomass. Above ground biomass was then dried at a temperature of 84 °C for 48 h and pods were dried at a temperature of 37 °C for two weeks. Canopy biomass and pod mass were then weighed and recorded.

Due to limitations on available space, the experiments were confined to a 2 m^2 plot, measuring 1 m × 2 m. The area was split into two plots, where high density and low density experiments were conducted. In each case plants were planted in uniform grid type arrangements and planting distances chosen to ensure interactions between each plant and its neighbours occurred in each case. In the low density experiment, the 1 m^2 was filled with 9 plants arranged in a 3 × 3 arrangement with $D_r = 0.4$ m and $D_c = 0.3$ m. In the high density experiment, another 1 m^2 was filled with 16 plants arranged in a 4 × 4 arrangement with $D_r = 0.25$ m and $D_c = 0.25$ m.

This data was used to inform the carrying capacity k_h by taking the maximum plant height of all plants in the experiments. The parameters α_g, b_g and c_g were determined by taking least-squares fits of the experimental data against model simulations. The average dry canopy biomass and pod mass at harvest for the high and low density arrangements can be found in Table 1. There is a clear difference in both average pod mass and canopy biomass at harvest between the two planting densities.

To apply the model described in this paper to other crop species that form a canopy, it would be necessary to provide values for all of the parameters in Table 2, (except for k_i, which is the incoming radiation and is fixed). For plants that do not reach full height early in their development, it may also be necessary to adapt the height equation to include the effect of competition on height.

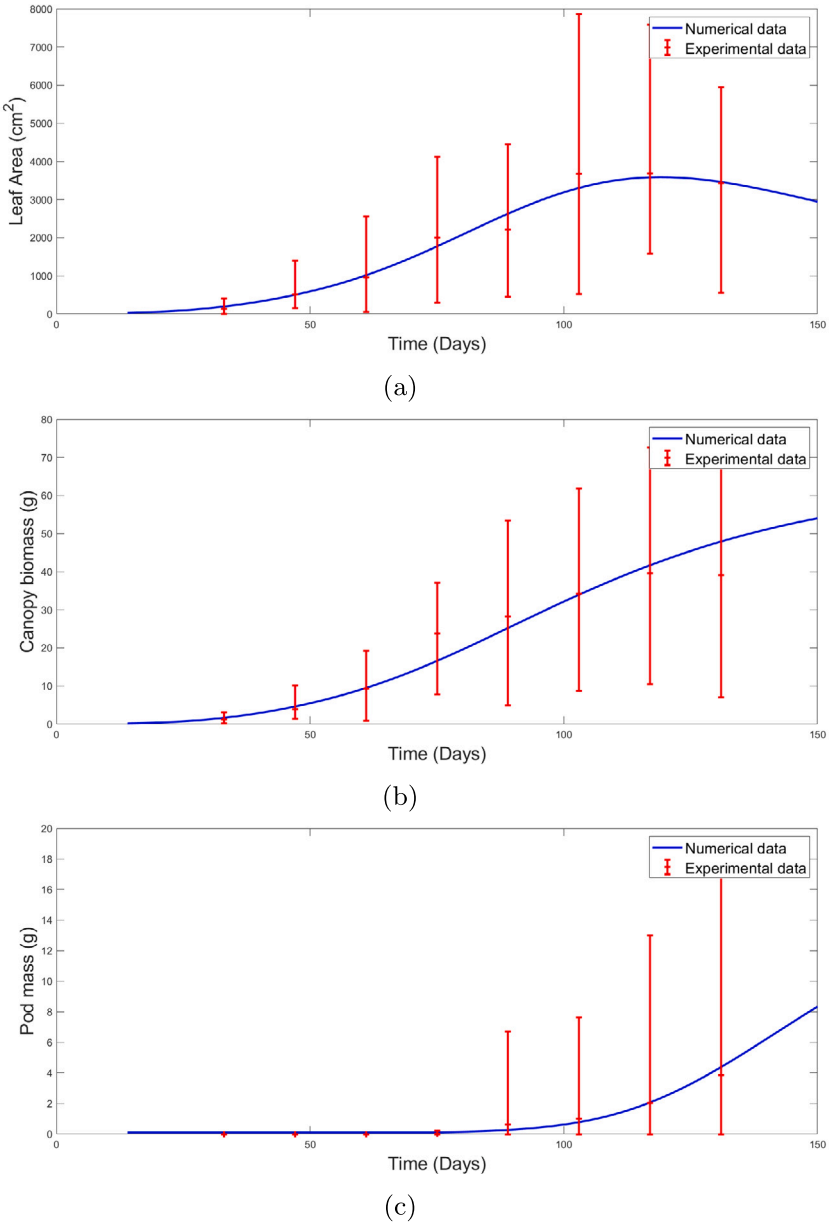

Fig. 7. The simulated (a) leaf area, (b) canopy biomass and (c) pod mass compared with the experimental data for the species Uniswa Red, using the non data-fitted case of a temperature of 23 °C. Red bars indicate the upper and lower bounds of the experimental data.

Table 1
The average canopy biomass and pod mass for plants of the species Uniswa Red grown at the temperature 28 °C for planting densities of 9 plants per square metre and 16 plants per square metre for the FCG experiments.

	Canopy Biomass (g)		Pod Mass (g)		Total biomass	
Plants per square metre	Average mass	Standard deviation	Average mass	Standard deviation	Average mass	Standard deviation
9	65.82	15.64	36.71	10.77	102.53	24.06
16	33.46	9.75	20.43	4.60	53.89	13.22

6. Numerical simulations

We now compare the mathematical model described by Eqs. (41) to (45) for a greenhouse crop of 9 plants with the available experimental data detailed in Section 5. For these comparisons, parameters for all plants are considered equal and the only difference between plants is the overlap incurred by their position. Leaf area, canopy biomass and pod mass are available for the TCRU experimental data, and ground cover data is provided with the FCG experiments. These two experiments have different planting layouts, both of which are illustrated in Fig. 5. For each case, simulated data is averaged over all N plants and compared to the corresponding mean average of the experimental data. Temperature was constant for each simulation and a range of temperatures were investigated, corresponding to those in the TCRU experiments (23 °C, 28 °C and 33 °C).

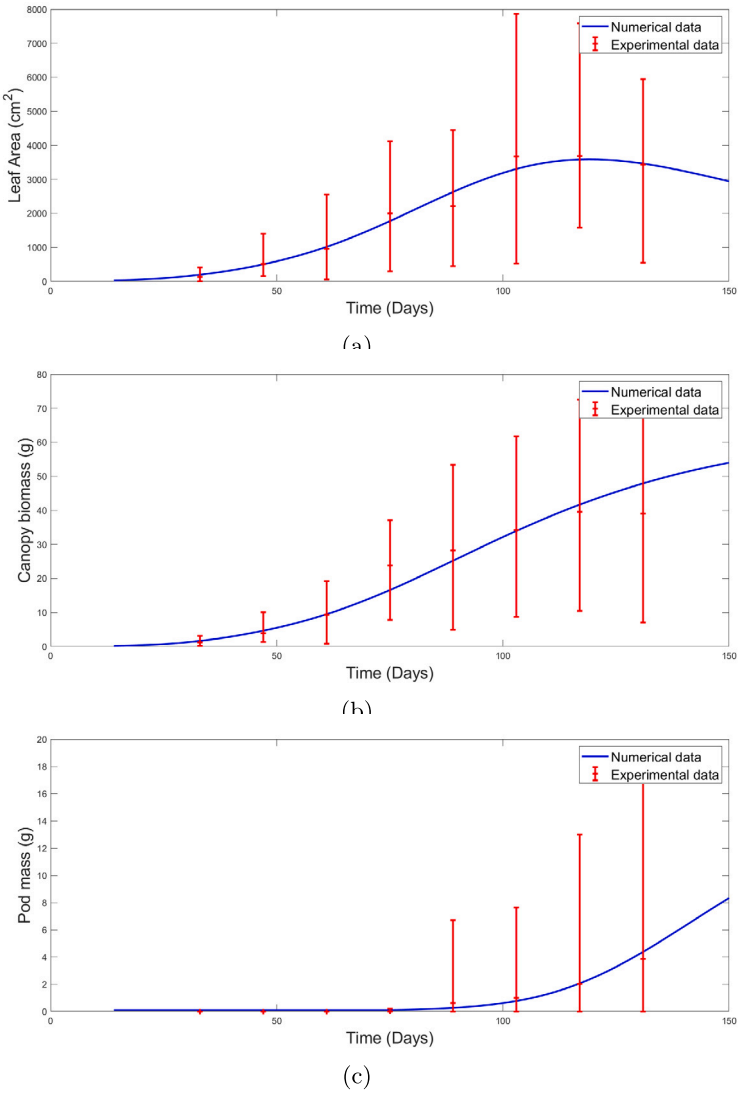

Fig. 8. The simulated (a) leaf area, (b) canopy biomass and (c) pod mass compared with the experimental data for the species Uniswa Red, using the non data-fitted case of a temperature of 33 °C. Red bars indicate the upper and lower bounds of the experimental data.

A simulation of leaf area, canopy biomass and pod mass compared to experimental data for Uniswa Red at 28 °C is shown in Fig. 6. This is the data set used to fit the model parameters for Uniswa Red and is hereby referred to as the 'fitting case'. The two non-fitted cases of 23 °C and 33 °C are given in Figs. 7 and 8, respectively. A comparison of the evolution of ground cover over time and experimental data is given in Fig. 9. Plants are arranged as in Fig. 5(b) for a temperature of 28 °C and parameters given in Table 2.

The simulations of Uniswa Red show a good fit to the experimental data for all three temperatures, with the average pod mass being within the minimum and maximum of the experimental data for all 8 data points. Although not shown here, we also find a good fit to the experimental data for S19-3, which can be found in Appendix.

The mean absolute error (MAE) and the Nash–Sutcliffe efficiency (NSE) value (Nash and Sutcliffe, 1970) for these simulations are given in Tables 4 and 5 for both Uniswa Red and S19-3. The NSE indicates how well a plot of the experimental versus the simulated data fits the 1:1 line; where NSE $\in [-\infty, 1]$ (Nash and Sutcliffe, 1970). A value of 1 would indicate a perfect model and a value equal to or less than 0 would indicate that the model is no better at predicting plant growth than taking an average of the experimental data. The results mostly show a very good fit to data, with NSE values close to 1. The exception is S19-3 leaf area at 23 °C with an NSE value of 0.13. It should be noted that for this case, experimental data is fairly flat, and so the low NSE value is an indication that taking the average of all data gives a good fit, rather than indicating that our model gives a bad fit. In fact, the MAE is low compared to S19-3 leaf area at 33 °C.

7. Model exploration

In this and subsequent sections we explore the behaviour of our multiscale mathematical model. We begin with a sensitivity analysis in Section 7.1, where we focus on the sensitivity of ground cover to variations in the magnitude of key mechanisms. It is found that increasing the size of a canopy can benefit overall plant growth until a critical point is reached at which increased competition for light outweighs the benefits of increased sunlight capture. We then consider how individual plant position impacts the yield of an individual plant in Section 7.2. Finally, the impact that variation in model parameters between plants has on total yield is discussed in Section 7.3.

7.1. Sensitivity analysis

We conducted a local sensitivity analysis, varying each parameter in turn, up to 10-fold above and below the values reported in Table 3. We

Table 2
Table of dimensional parameter values. For parameters that are species specific, * denotes the species S19-3 and † denotes Uniswa Red.

Parameter	Value	Unit	Description	Source
α_h	0.75	d^{-1}	Plant height growth rate	This study
k_h	30*, 25†	m	Plant height carrying capacity	This study
d_h	0.02	d^{-1}	Plant height decay rate	This study
T_{opt}	30*, 28†	°C	Optimum growth temperature	Karunaratne (2009)
T_{crit}	12*, 8.5†	°C	Critical temperature for growth	Karunaratne (2009)
T_{ceil}	45*, 38†	°C	Maximum temperature for plant growth	Karunaratne (2009)
ω	0.7*, 1†	–	Temperature Stress	This study
a	0.19*, 0.21†	d^{-1}	Maximum leaf growth rate	Data fitted
b	67.74*, 92.0†	d	Time of peak leaf accumulation	Data fitted
c	28.78*, 38.00†	d	Time window of significant leaf accumulation	Data fitted
d_L	1.37×10^{-2}*, 1.6×10^{-2}†	d^{-1}	Leaf decay rate	Data fitted
L_A	3.9×10^{-3}*, 3.0×10^{-3}†	m^2	Leaf area per leaf	TCRU experimental data (Karunaratne, 2009)
PAR	0.5	–	Fraction of photosynthetically active radiation	Cornelissen (2005)
k_i	16	MJ m^{-2} d^{-1}	Incoming radiation	Met office (2016)
c_e	1.87*, 2.04†	gMJ^{-1}	Mass accumulation efficiency rate	Data fitted
κ	0.6	–	Extinction coefficient	Karunaratne (2009)
k_{max}	180.66*, 161†	g	Canopy biomass carrying capacity	TCRU experimental data (Karunaratne, 2009)
d_c	1×10^{-3}*, 5×10^{-4}†	d^{-1}	Canopy biomass decay rate	Data fitted
α_g	53.85*, 103.33†	d^{-1}	Ground cover growth rate	Data fitted
b_g	17.04*, 14.00†	d	Time of peak ground cover growth	Data fitted
c_g	21.67*, 30.00†	d	Window of significant ground cover growth	Data fitted
h_0	0.05	m	Plant height at emergence	This study
L_0	1	–	Leaf number at emergence	This study
G_0	L_A	m^2	Ground cover at emergence	This study
c_0	0.24*, 0.19†	g	Canopy biomass at emergence	This study

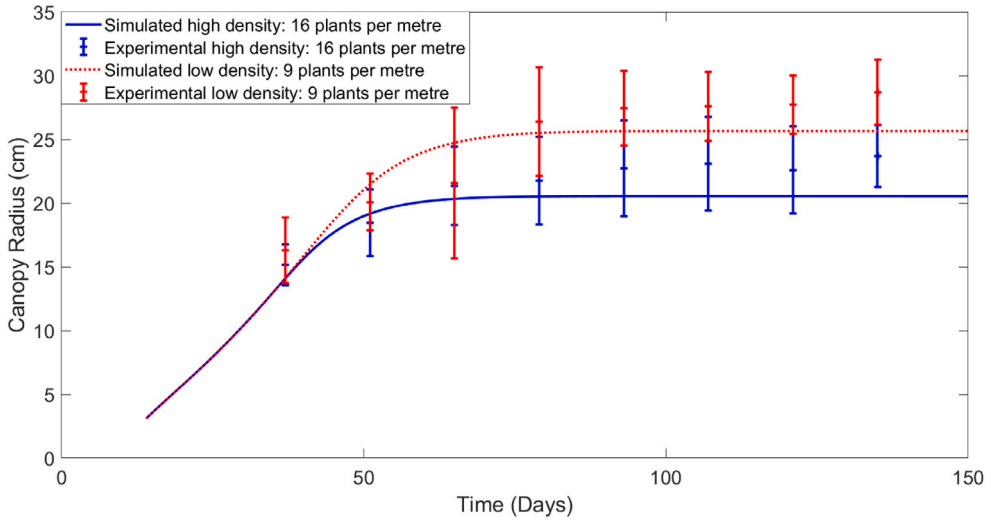

Fig. 9. The simulated canopy radius of two density treatments of 9 plants per square metre and 16 plants per square metre. Here ground cover is described by Eq. (10), temperature is 28 °C and individual plant arrangements with respect to each other and plant borders can be found in Fig. 5(b). The parameter values for this simulation are given in Table 2.

Table 3
Table of non-dimensional parameters and the corresponding expressions.

Parameter	Expression
$\bar{d}_h$	d_h/α_h
$\bar{\alpha}_L$	$aT_{eff}/L_A\alpha_h$
$\bar{b}$	$\alpha_h b$
$\bar{c}$	$\alpha_h c$
$\bar{d}_L$	$d_L T_{sl}/\alpha_h$
$\bar{\alpha}_g$	α_g/α_h
$\bar{b}_g$	$\alpha_h b_g$
$\bar{c}_g$	$\alpha_h c_g$
$\bar{\alpha}_c$	$R_0 c_e L_A/c_0\alpha_h$
κ	κ
K_c	c_0/k_{max}
$\bar{d}_c$	$d_c T_{sc}/\alpha_h$
$\bar{\alpha}_P$	$\alpha_P c_0$
$\bar{d}_P$	d_P/α_h

Table 4
The mean absolute error (MAE) and the Nash–Sutcliffe efficiency (NSE) value for the leaf accumulation model's prediction of canopy biomass and leaf area for Uniswa Red and S19-3 when compared to the TCRU experimental data.

Temperature	Canopy biomass (g)				Leaf Area (cm^2)			
	Uniswa Red		S19-3		Uniswa Red		S19-3	
	MAE	N-S	MAE	N-S	MAE	N-S	MAE	N-S
23 °C	2.83	0.85	4.57	0.73	168.05	0.84	366.33	0.13
28 °C	3.05	0.97	2.67	0.95	101.80	0.99	39.79	0.996
33 °C	2.78	0.92	2.95	0.94	160.94	0.97	499.74	0.74

quantitatively measured, primarily, the effect of parameter variation on the leaf area, canopy biomass and pod mass at the expected time of harvest (i.e. 150 days), whilst also looking for significant variations in growth behaviour over time for leaf area, ground cover, canopy biomass and pod mass. Varying the model parameters up to 10-fold allows us to explore the robustness of the model to changes greater

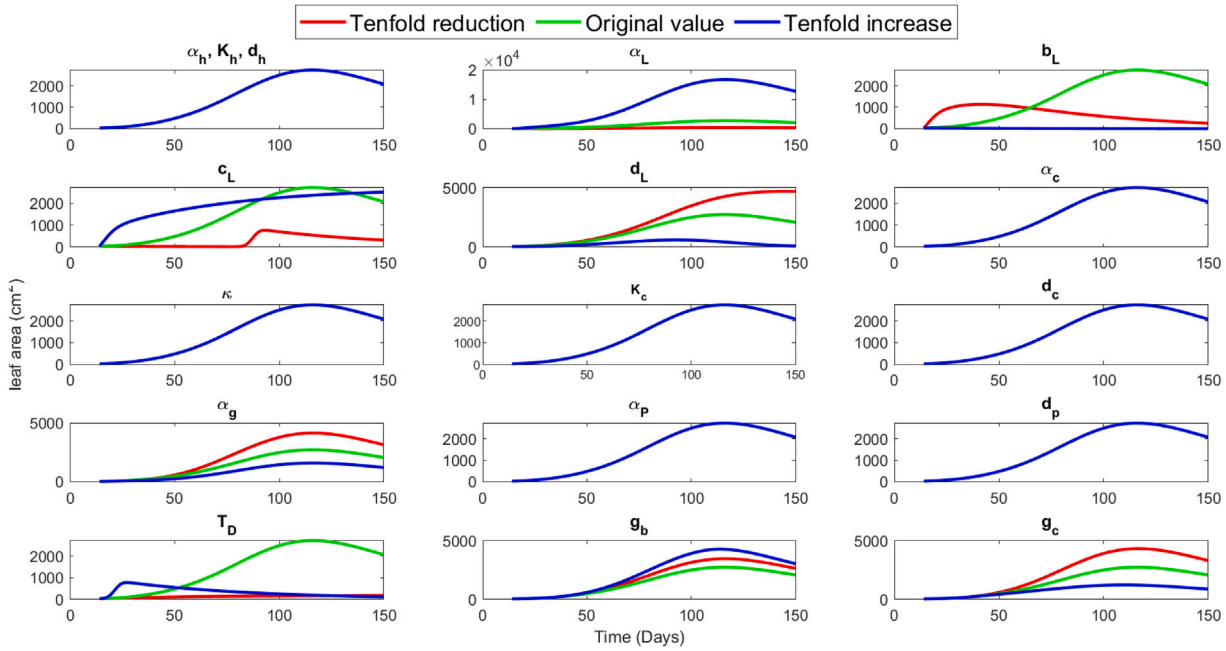

Fig. 10. Development of leaf area over time with a tenfold increase and tenfold decrease to each non-dimensional parameter in turn. The base-case parameters of this analysis were for Uniswa Red at 28 °C.

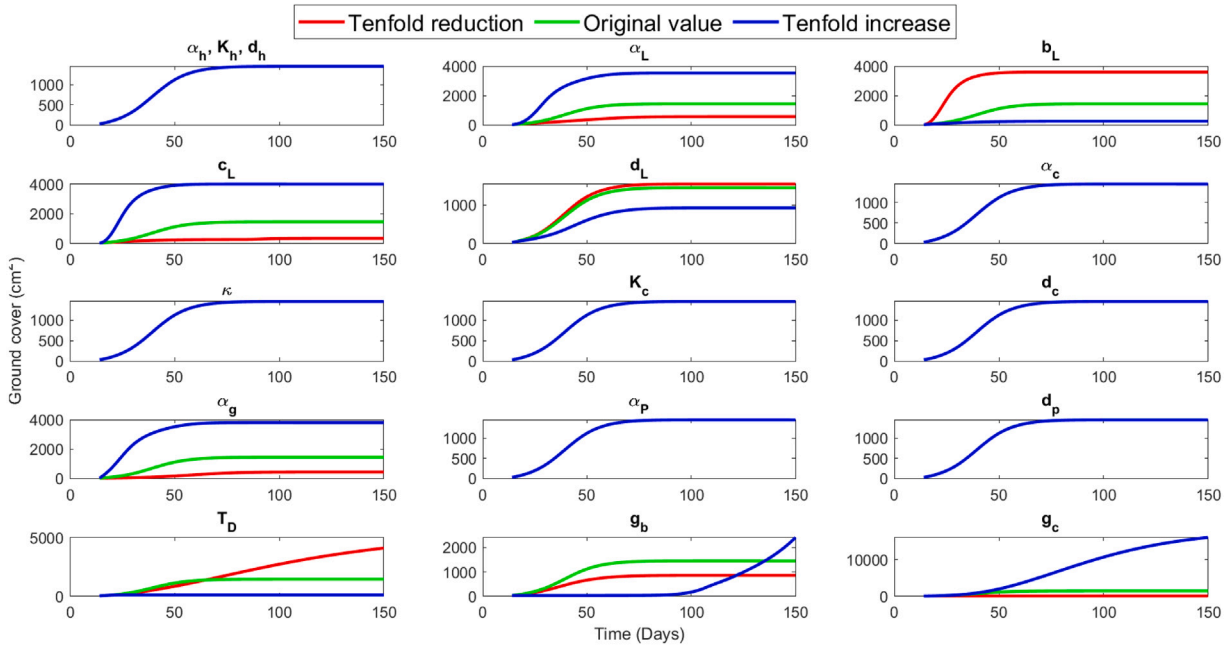

Fig. 11. Development of ground cover over time with a tenfold increase and tenfold decrease to each non-dimensional parameter in turn. The base-case parameters of this analysis were for Uniswa Red at 28 °C.

Table 5
The mean absolute error and the Nash–Sutcliffe value for the prediction of pod mass for Uniswa Red and S19-3 when compared to the TCRU experimental data.

Temperature	Uniswa Red		S19-3	
	MAE	N-S	MAE	N-S
23 °C	0.65	0.95	0.86	0.92
28 °C	0.56	0.995	1.05	0.98
33 °C	0.2	0.96	0.84	0.99

than those biologically feasible thereby ensuring all possible effects have been explored. The base-case parameters of this analysis were for Uniswa Red at 28 °C. Variations in parameters were applied to all plants equally and so in every simulation that follows, the only difference between plants is that incurred by its position. This analysis is only valid for the planting distance used in this study of 0.2 m and 0.35 m for rows and columns, respectively.

Figs. 10 to 13 shows the development of leaf area, ground cover, canopy biomass and pod mass for a tenfold increase and tenfold decrease to each non-dimensional parameter in turn.

Changes to parameters ascertaining to plant height, namely α_h, K_h, and d_h, do not change leaf area, canopy biomass and pod mass. This

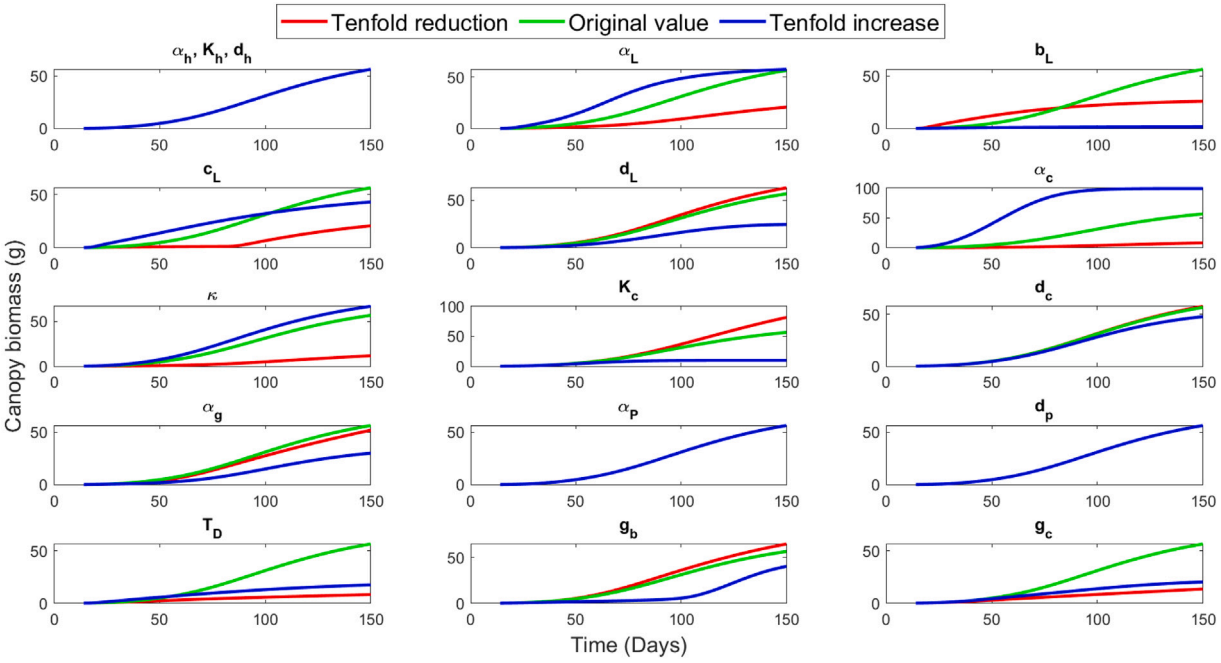

Fig. 12. Development of canopy biomass over time with a tenfold increase and tenfold decrease to each non-dimensional parameter in turn. The base-case parameters of this analysis were for Uniswa Red at 28 °C.

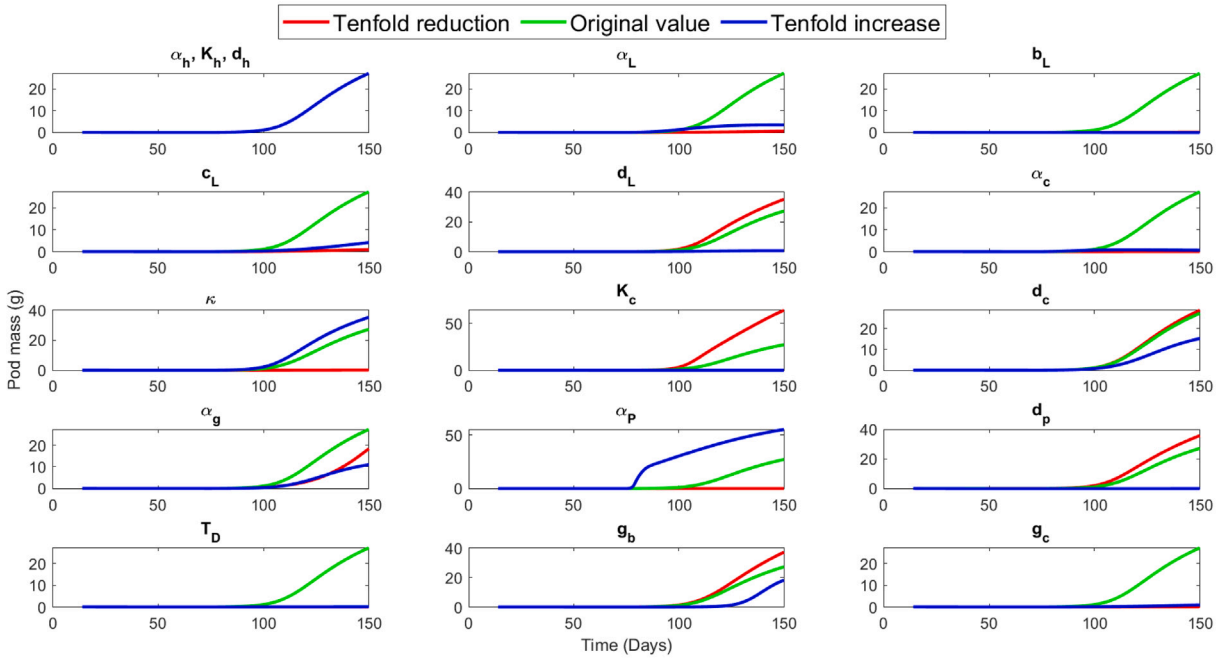

Fig. 13. Development of pod mass over time with a tenfold increase and tenfold decrease to each non-dimensional parameter in turn. The base-case parameters of this analysis were for Uniswa Red at 28 °C.

is because relative height, not absolute height affects these variables. Since changes to plant parameters impacts all plants equally then all plants remain at the same height.

Changes to maximum growth rate for leaf area α affects leaf area (Fig. 10) as expected; a tenfold increase will increase the maximum leaf area and a tenfold decrease will decrease maximum leaf area. This in turn will impact ground cover (Fig. 11) so that increases to α will increase ground cover and decreases to α will decrease ground cover. The canopy biomass (Fig. 12) growth rate is a function of α. An increase in α will allow canopy biomass to reach its carrying capacity faster. Conversely, decreasing α will prevent canopy biomass reaching the carrying capacity in the window of peak leaf growth. Both of these cases cause a decrease to pod mass (Fig. 13), since the canopy growth rate within the podding phase impacts the pod growth rate. For an increase in α the plant is already very close to carrying capacity when the podding phase is initiated and therefore more resource is being partitioned to canopy growth to the detriment to pod development. A decrease in α causes the leaf area to decrease and so too the canopy biomass growth rate and therefore total pod mass.

The time of maximum leaf accumulation is given by b. A reduction in b causes a larger leaf area (Fig. 10) at the initial stages of growth, this is behaviour to be expected intuitively, however overall leaf area

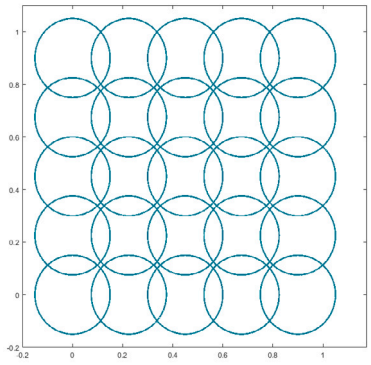

(a) Uniform Grid.

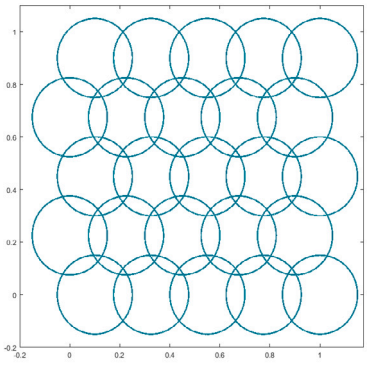

(b) Indented Grid 1.

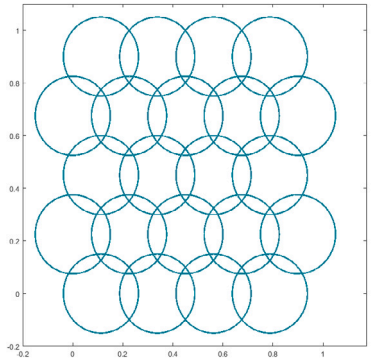

(c) Indented Grid 2.

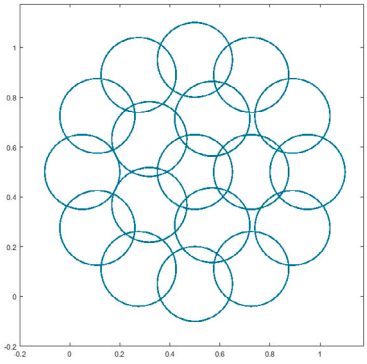

(d) Circular Layout.

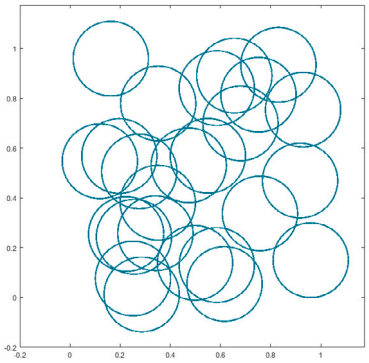

(e) One example of a Random Layout.

Fig. 14. A birds-eye schematic of five planting layouts in a 1 m^2 plot with planting distance D = 0.225 m. (a) Uniform Grid (plants are evenly spaced). (b) Indented Grid 1 (every other row is indented by the amount of excess space between the row end and 1 m^2 boundary (0.1 m)). (c) Indented Grid 2 (every other row is indented by half the planting distance (0.1125 m) where this amount of indentation causes one plant of every other row to be excluded) (d) Circular Layout (plants are arranged in rings of increasing diameter around a central plant). (e) Random Layout (here the number of plants is fixed so that N would be equal to the number of plants in the Uniform Grid case).

reduces for both, increases and decreases to b. Decreasing the time of peak growth by as much as tenfold causes a large part of the significant growth window, to occur before germination. Similarly, a tenfold increase in b will cause the window of peak growth to occur after the plant has reached maturity. Thus, the plant will not accumulate as much total leaf area in the 150 days for which we are observing. Regarding ground cover (Fig. 11), a reduction in b will cause a larger leaf at the initial stages of growth, which incidentally is the peak growth time of ground cover. This would cause the plant to spread wider, faster. This has the knock on effect that there is more overlap, and so canopy biomass (Fig. 12) are detrimentally affected. When it comes to pod development (Fig. 13), its growth rate is dependent on the canopy biomass growth rate. Therefore, once canopy biomass has reached its carrying capacity, pod development stops. A decrease in b causes canopy biomass to reach its competition-dependent carrying capacity faster.

This analysis was repeated with a tenfold increase in planting distance. This allows us to see the impact of changing b in a system

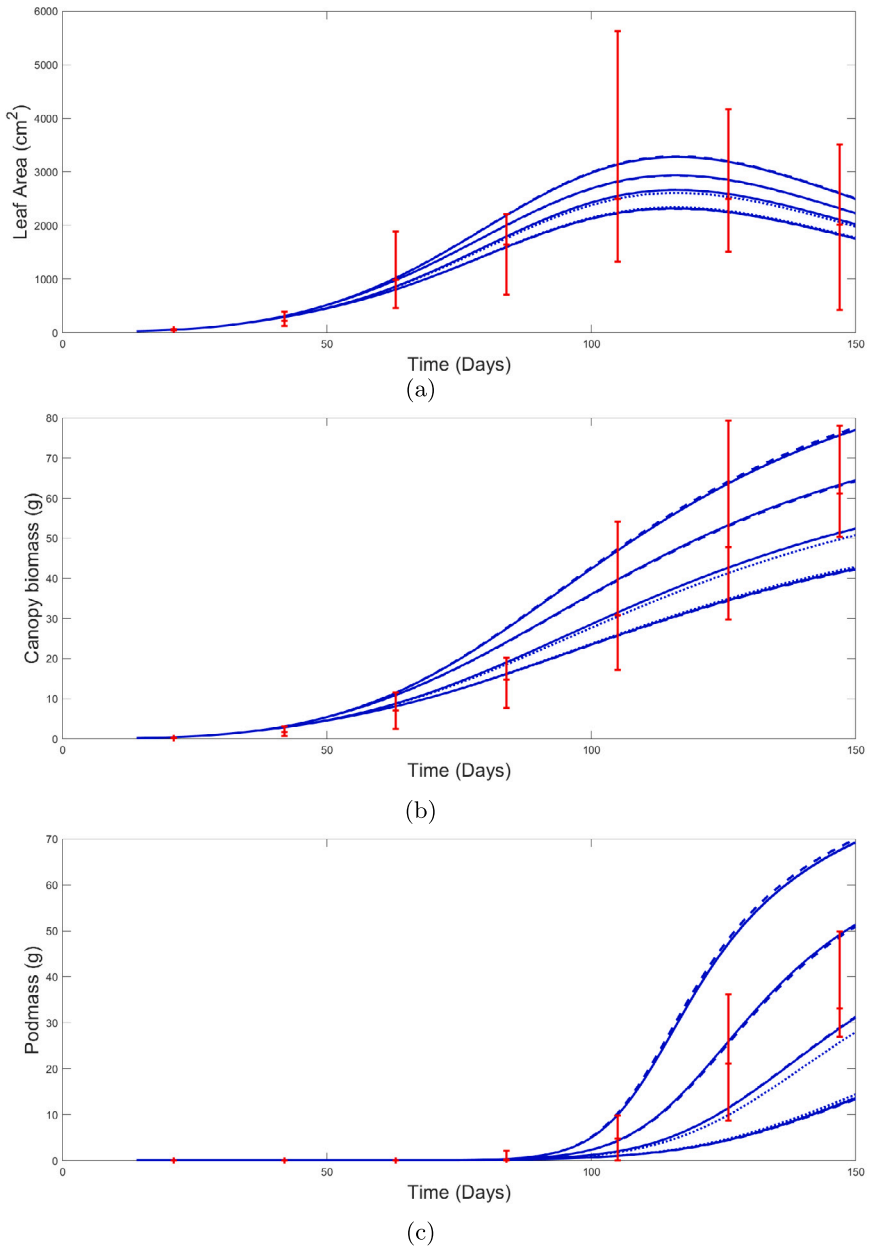

Fig. 15. Simulations of fifteen plants of the species Uniswa Red grown at a temperature of 28 °C compared with the TCRU and FCG experimental data. Here (a) is the leaf area, (b) is the canopy biomass and (c) is the pod mass. The system is described by Eqs. (41)–(45) and parameters are assumed equal between plants as stated in Table 2. Each simulated plant is initiated at day 14 (the estimated time of emergence) and assumed to have a canopy comprising of one leaf at this point. Plants are arranged in a five by three grid, where the distance between plants in a row is 0.2 m and the distance between rows is 0.35 m. Red bars indicate the upper and lower bounds of the experimental data.

with less competition. When b is decreased tenfold, the canopy biomass decreases by 53.9% for the default planting arrangement compared to 23.2% for the less dense planting arrangement. This clearly demonstrates the negative impact of increased spreading on biomass, caused by the earlier onset of leaf development. It also shows that when both planting distance and b are increased tenfold, some competition still occurs.

Pod mass decreases by 99.4% with a tenfold increase to b compared to 99.97%, when planting distance is increased tenfold. Increasing b means that the peak leaf development occurs much later and severely impacts biomass and therefore pod development. Whilst it appears it affects the less dense layout more, the pod mass (using default parameters) gives a larger yield for the less dense arrangement. The pod mass for increased b is exactly the same for both arrangements, because no competition occurs in either arrangement.

A reduction in c causes the window of peak growth to shorten. Intuitively, this implies that total leaf growth reduces. This can be seen in Fig. 10, however we also see a sudden bump in growth at approximately 90 days. This is because, shortening the window of significant growth by tenfold causes all growth to occur almost instantaneously when time is approximately equal to b (in this case at 92 days). The reduced leaf area causes reductions to ground cover (Fig. 11), canopy biomass (Fig. 12) and pod mass (Fig. 13). An increase to c causes the window of peak growth to increase and so it could be expected that total leaf area would increase. In Fig. 10 we see that there is a more leaf growth at the initial stages, however closer to maturation, the maximum leaf area for the original parameter values is larger than for a tenfold increase in c. By observing Fig. 11 we can see that the larger leaf area at the initial stages of growth causes a larger ground cover and thus more overlap. The additional overlap is what prevents the

plant increasing its maximum leaf area to more than for the original parameters. We also find, that although increasing leaf area increases biomass and pod mass growth, the detrimental impact of the added overlap decreases overall canopy biomass and pod mass values. When we increase the planting distance we find that this behaviour changes. Canopy biomass decreases by 23.7% with a tenfold increase in c, this is compared to an increase of 24.1% when planting distance is increased. This is because with reduced competition, a longer period of leaf development is beneficial for canopy biomass. Podding mass decreases by 84.6% for the default planting density and by only 1.6% for the reduced planting density. This shows that although canopy biomass has increased, because it is reaching steady state earlier with the original c value, pod mass is negatively affected.

A reduction in d_L causes an increase to leaf area (Fig. 10), which could have been intuitively predicted as a reduction to d_L would imply a reduction to leaf senescence. Conversely an increase in d_L causes a decrease in leaf area. The impact that increasing d_L has on ground cover (Fig. 11) is significantly larger than when decreasing d_L.

Leaf area is unaffected by parameters relating to canopy biomass and pod mass, i.e. α_c, κ, K_c, d_c, α_P and d_P, therefore when discussing these parameters we will only consider canopy biomass and pod mass.

Changes to α_c impact the time it takes the canopy to reach its carrying capacity. Thus a tenfold increase causes canopy biomass (Fig. 12) to reach carrying capacity at 100 days, whereas a tenfold decrease will mean that canopy growth increases so slowly that it does not reach carrying capacity before leaf growth ceases. This means that if the plant reaches carrying capacity before podding initiates then no biomass will be partitioned to pods (Fig. 13). This is for a tenfold increase in α_c. If there are smaller increases, pod mass will increase until a critical point at which it will begin to be negatively affected. For a decrease in α_c pod mass decreases.

The leaf position is determined by κ, which ranges between 0 and 1. Therefore instead of applying a tenfold increase, we set $\kappa = 1$. Increasing κ implies a plant with horizontally positioned leaves that are more efficient at capturing sunlight, thus an increase in biomass can be seen (Fig. 12). The increase in biomass acquisition has not caused the plant to reach a carrying capacity before maturation and so pod accumulation has not decreased (Fig. 13). We instead see an increase in pod mass demonstrating the previous conviction that for some amount of increase to biomass growth rate, there will be an increase in pod mass until a critical point when pod growth will be negatively impacted. A decrease in κ implies vertically positioned leaves. Since our model only considers radiation from a stationary source directly above the canopy, vertically positioned leaves implies less sunlight capture. This leads to a decrease in biomass accumulation and also pod mass growth.

An increase in K_c is equivalent to decreasing canopy biomass carrying capacity, for which we see a decrease in canopy biomass (Fig. 12) and therefore pod mass (Fig. 13). Due to the magnitude that the carrying capacity is decreased, canopy biomass meets the carrying capacity before pod initiation and therefore there is no pod growth for a tenfold increase to K_c. A decrease in K_c is equivalent to an increase in canopy biomass carrying capacity, for which we see an increase to canopy biomass and therefore pod mass.

A decrease in d_c would imply a decrease in biomass senescence, which causes as increase to biomass (Fig. 12) and therefore pod mass (Fig. 13). An increase to d_c would imply more biomass decay and therefore causes a decrease to biomass and pod mass.

An increase in the maximum ground cover spreading rate, α_g, causes the plant to occupy a larger space and therefore cause a larger amount of competition. This decreases leaf area (Fig. 10), canopy biomass (Fig. 12) and pod mass (Fig. 13). If α_g was to increase a little, leaf area will always decrease when plants are arranged at this density, as the only relationship ground cover has on leaf area is via competition. With an increased planting distance, small changes to α_g will have no effect. The effect increased ground cover has on canopy biomass can be both positive and negative. A large surface area means more canopy can absorb radiation, which has a positive impact, however more competition has a negative impact. Therefore, increases to α_g are beneficial to yield until a critical point where further increases has a detrimental impact. Clearly, at this planting density a tenfold increase to α_g exceeds the critical point causing canopy biomass to decrease by 46.6%. If planting distance increases tenfold, we find that canopy biomass increases by 3%. Decreases to α_g causes less competition and so increases leaf area, however decreases canopy and pod growth.

Pod mass growth and decay rate, denoted by α_P and d_P, respectively relate only to pod mass. An increase to pod growth rate α_P causes an increase in pod mass (Fig. 13). An increase to d_P causes a decrease to pod mass. Conversely, decreases to α_P implies a decrease to canopy biomass and a decrease to d_P causes an increase to pod mass.

Changes to T_{eff} equate to changes in the number of degreedays accumulated in one day. By increasing T_{eff}, a similar impact to decreasing b_L can be seen in that the time of peak growth occurs so early that a large proportion of the growth window is cut off. Similarly, decreasing T_{eff} causes the time in days to reach peak growth to increase. In the case of a tenfold increase, this implies that it does not reach peak growth in the 150 day time window.

Changes to b_g causes the time at which peak canopy spreading occurs. An increase causes peak spreading to occur when leaf area is larger causing ground cover to become much larger (Fig. 11). This would only be the case until a certain point after leaves start senescencing faster than they accumulate. Although ground cover becomes larger, it is significantly smaller for the duration of the simulation window. We then find that there is less overlap before 100 days and so leaf area is larger (Fig. 10). Canopy biomass is much smaller, as although there is less competition, there is also less canopy to absorb radiation (Fig. 12). Pod mass is then similarly reduced. By decreasing b_g peak canopy spreading occurs at a much lower leaf area and so grows to a much smaller final size (Fig. 13). Thus, there is less competition and so leaf area is increased. In this case the trade off between increased canopy size and increased competition is such that canopy biomass, and therefore pod mass, has increased.

Increasing the time window of peak canopy spreading significantly increases ground cover. The extent is such that competition is increased so dramatically that leaf area, canopy biomass and pod mass are significantly affected. Decreasing c_g causes ground cover to be much smaller and thus decreasing competition causing an increase to leaf area. In this case the trade off between canopy size and competition is such that canopy biomass, and therefore pod mass, are also reduced. However in this case, the trade off is opposite for increases to b_g.

A summary of this investigation is given in Table 6. Here the qualitative impact of a tenfold change to parameter values is given for a planting distance of 0.2 m and 0.35 m between rows and columns and a planting distance of 2 m and 3.5 m between rows and columns. Changes to plant parameters have a predictable qualitative and quantitative effect on plant growth. In addition, this investigation has demonstrated the sensitivity between the plant and the crop, whereby increases to specific individual plant traits (increasing canopy size) has a detrimental effect on the total crop yield if competition occurs.

7.2. The effect of planting arrangement on crop yield

The form of our model allows us to investigate the effect that individual plant size and position has on the overall population. In this section we begin by investigating the impact of plant position on the yield of an individual plant, at a temperature of 28 °C although the results also apply at 23 °C and 33 °C. In order to do this we consider the planting arrangement given in Fig. 5(a) before proceeding to consider the effect of different planting arrangements, as shown in Fig. 14. In each case variation in leaf area, canopy biomass and pod mass of each plant is used to examine the effect that different planting arrangements have.

Table 6
Summary of local sensitivity analysis results after a tenfold increase and tenfold decrease to parameter values. Results for the simulations using the default planting distance are shown in addition to results with a tenfold increase to planting distance.

Parameter	% change to total crop yield			
	Default planting distance		Increased planting distance	
	Tenfold decrease	Tenfold increase	Tenfold decrease	Tenfold increase
α_h	0	0	0	0
α	−97.6	−87.1	−98.7	−99.4
b	−99.4	−99.9	−93.9	−100
c	−96.3	−84.6	−99.1	−1.6
d_L	28.8	−97.4	15	−96.4
α_c	−99.6	−97.3	−99.1	−98.8
κ	−99.3	29.6	−98.1	12.6
K_c	134.6	−99.8	94.6	−100
d_c	5.5	−44.2	1.8	−15.8
α_g	−32.5	−59.5	−75.3	1.9
α_P	−99.7	102.8	−99.8	11.3
d_p	31.6	−99.9	6.7	−80.3
T_{eff}	−99.7	−99.5	−99.2	−99.9
b_g	36.5	−33.1	−16.7	−36.9
c_g	−99.5	−96.3	−99.9	−14.8

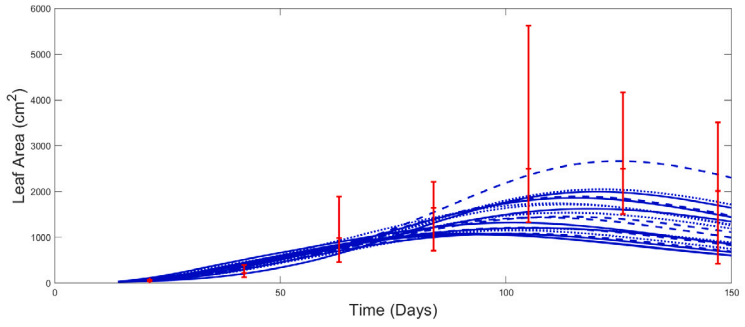

(a) Leaf area

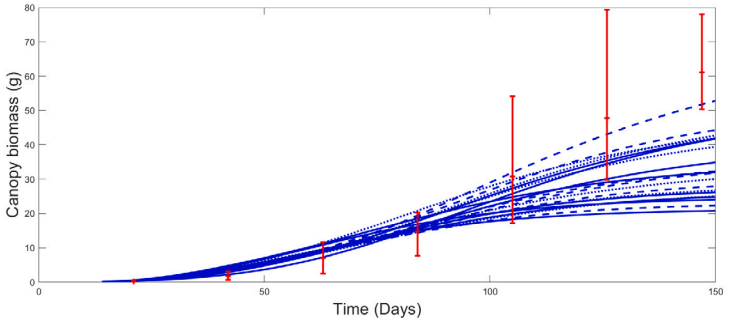

(b) Canopy biomass

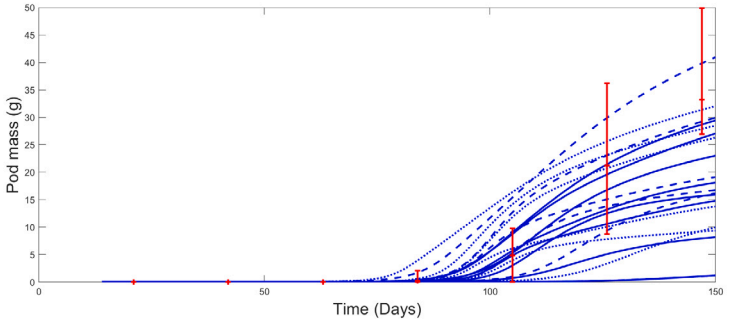

(c) Pod mass

Fig. 16. Twenty simulations of the mean total: (a) leaf area; (b) canopy biomass; and (c) pod mass of a crop of 15 plants grown according to the Uniform Grid arrangement of Fig. 1(a), at a temperature of 28 °C compared with experimental data for Uniswa Red. All plant parameters have been randomly varied following that of a normal distribution. Red bars indicate the upper and lower bounds of the experimental data.

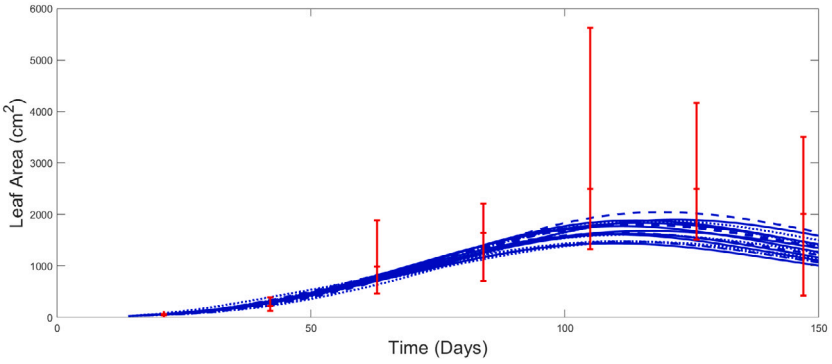

(a) Leaf area

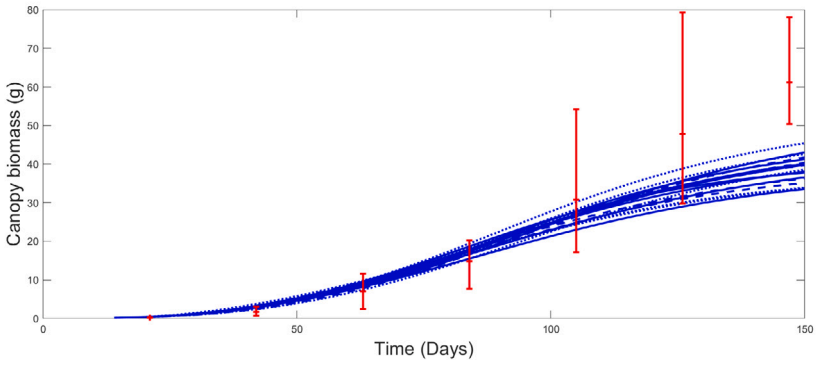

(b) Canopy biomass

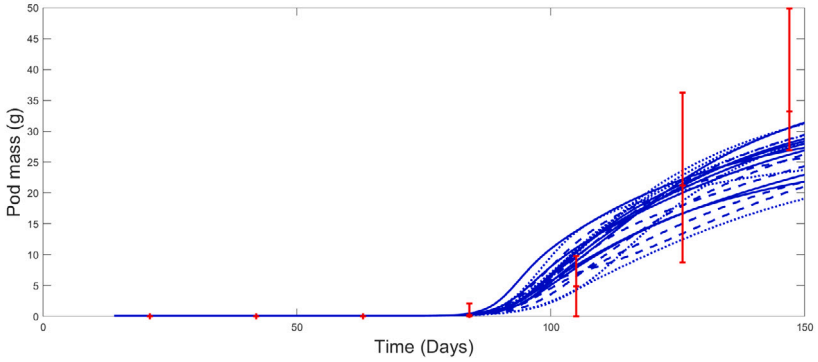

(c) Pod mass

Fig. 17. Twenty simulations of the mean (a) leaf area (b) canopy biomass and (c) pod mass compared with the experimental data for Uniswa Red. All plant parameters, but those ascertaining to height and ground cover growth rate, are randomly varied. Red bars indicate the upper and lower bounds of the experimental data.

7.2.1. Uniform grid arrangement

The simulated growth of fifteen plants arranged as in Fig. 5(a) is compared to experimental data (TCRU and FCG) in Fig. 15. In both the TCRU and FCG experiments plants were arranged in a uniform grid. Due to the destructive nature of the data collection, the experimental data collected from the TCRU greenhouses could not be assigned to one particular plant over the duration of the experiment. As such, a specific plant position cannot be assigned to a piece of data and so the relationship between plant position and yield cannot be easily extracted. Instead, a simulation of the same layout has been conducted to investigate this relationship.

Parameters for all plants are assumed equal and so any difference between plants is incurred by the individual plant position. From Fig. 15 we can see that plant position has a clear impact on both leaf area and canopy biomass. Although not shown explicitly in Fig. 15, it can be found that, as one might expect, the inner three plants (those which interact with 9 neighbouring plants) have the lowest pod yield and the plants positioned on the corners (those which interact with three other plants) have the highest yield.

For leaf area the range of simulation data for the fifteen plants is within the bounds of the experimental data. For canopy and pod biomass however, the data for individual plants are not within the bounds of the experimental data, although the average of the data set is. Although the canopy biomass of individual plants is not necessarily within the upper and lower bounds of the data, we do see a similar magnitude of variation.

7.2.2. Different planting arrangements

The method of simulating plant growth described here also allows us to investigate how plant layout can affect total canopy biomass. Five

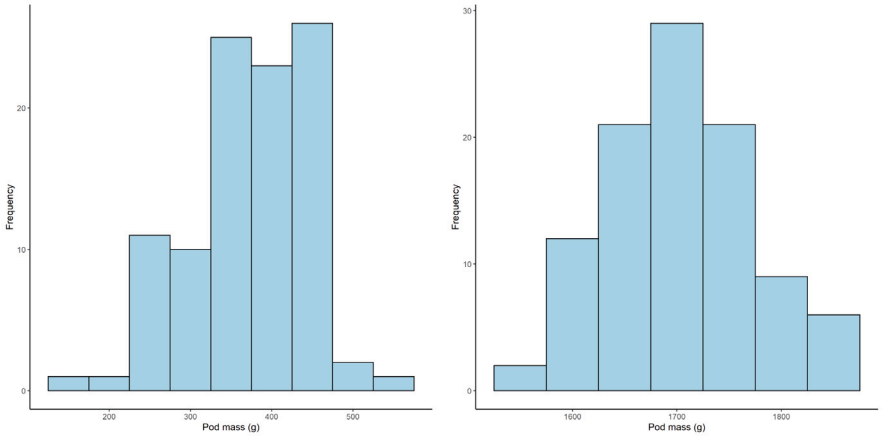

(a) Default planting distance (b) Increased planting distance

Fig. 18. Histograms showing yield modelling in 100 simulations with random variation to plant parameters. Figure (a) shows the distribution using the default planting density, whereas (b) shows the distribution with planting distance increased tenfold.

different planting layouts have been chosen, with a schematic of each layout given in Fig. 14. The layouts are as follows:

- Fig. 14(a) is a Uniform Grid, where plants are evenly spaced throughout the plot area;
- Fig. 14(b) is similar to the Uniform Grid, however here every other row is indented by the amount of excess space between the row ends and the edge of the plot area (Indented grid 1);
- Fig. 14(c) is another form of indented grid, where every other row is indented by half the planting distance (Indented Grid 2). The difference between this layout and the one shown in Fig. 14(b) is the extent of the indent. In this layout the amount of indent may cause plants at the end of indented rows to not fit in the plot area and are therefore excluded. In the previous layout, the indentation is such that plants are never excluded;
- Fig. 14(d) is a Circular layout where plants are arranged in rings with planting distance D between and within each ring; and
- Fig. 14(e) is a Random planting layout.

These five layouts have been chosen as they provide a good range of physically feasible examples.

To demonstrate the effect various planting arrangements have on the total canopy biomass we consider the case of planting in a 1 m^2 plot with an initial planting distance of $D = 0.225$ m. A planting distance of 0.225 m would cause a 0.1 m indent in Indented Grid 1 and an indent of 0.1125 m for Indented Grid 2. This allows a clear difference between the three grid arrangements. In contrast, a distance of 0.25 m would not allow any indentation in Indented Grid 1 and so there would be no visible difference between the Uniform Grid and Indented Grid 1. For the Random layout, plants are not restricted to a set planting distance and so instead, the number of plants is fixed so that N would be equal to the number of plants in the Uniform Grid Layout with planting distance D. The inbuilt MATLAB function randn is used to generate N random numbers from a uniform distribution for both the horizontal and vertical position of each plant within the plot area.

The species Uniswa Red has been chosen since canopy size data is available. A temperature of 28 °C is used as it is the optimum growth temperature for Uniswa Red. All plant parameters, including plant height parameters, are equal. This means that any difference in plant growth is incurred by the position in relation to other plants. We later investigate how variation in plant parameters affect yield. The simulations are run to 150 days for each layout illustrated in Fig. 14 and the total and average pod mass for all N plants can be found in Table 7.

We see that the Circular Layout gives the highest average pod mass per plant, but since the amount of plants that fit within the plot area is significantly fewer when compared to the other layouts, the total pod mass is less. The Random layout gives the worst average and total pod mass. The arrangement that maximises pod mass per square metre is Indented Grid 1, followed closely by the Uniform Grid. This is because these layouts have the most plants, whilst making the best use of the available space. This is particularly true for Indented Grid 1 which makes use of the empty space between row ends and the plot boundary. For this layout there is a 2.67 g pod mass deficit per plant when compared to the Circular Layout, but an extra seven plants. In contrast, the Random layout, which does not make good use of the available space has a 10.28 g pod mass deficit, so although there are seven more plants than the Circular Layout, it does not make up for the loss of biomass to the first eighteen plants. In a similar way, the increase in average canopy biomass does not make up for the decrease in N in Indented Grid 2.

Table 7
The average and total pod mass of N plants within a 1 m^2 plot with a distance between plants of 0.225 m.

Layout	Pod mass (g)		N
	Average	Total	
Uniform grid	22.78	569.51	25
Indented grid 1	24.17	604.28	25
Indented grid 2	25.57	562.67	22
Circular	26.84	483.05	18
Random	16.56	413.98	25

7.3. Investigating the effect of genetic diversity between plants

In addition to different planting positions, plants may also vary in their physiological behaviour, which is directly linked to their genetic makeup. In our model this diversity is directly linked to the model parameter values. In order to investigate the effect of such diversity, we now consider how variation in parameter values affects the average total leaf area, canopy biomass and pod mass of the crop. We assume that each plant parameter can be described by a normal distribution with the mean being the original value given in Table 2 and a variance being 10% of the mean. Without data, it is unclear if this level of variation is realistic and we find imposing just 10% variation has a significant effect.

A value is randomly selected from the distribution using the inbuilt MATLAB function randn and applied to each plant. Simulations were run twenty times for different random selections of each parameter. The results of all twenty simulations are given in Fig. 16.

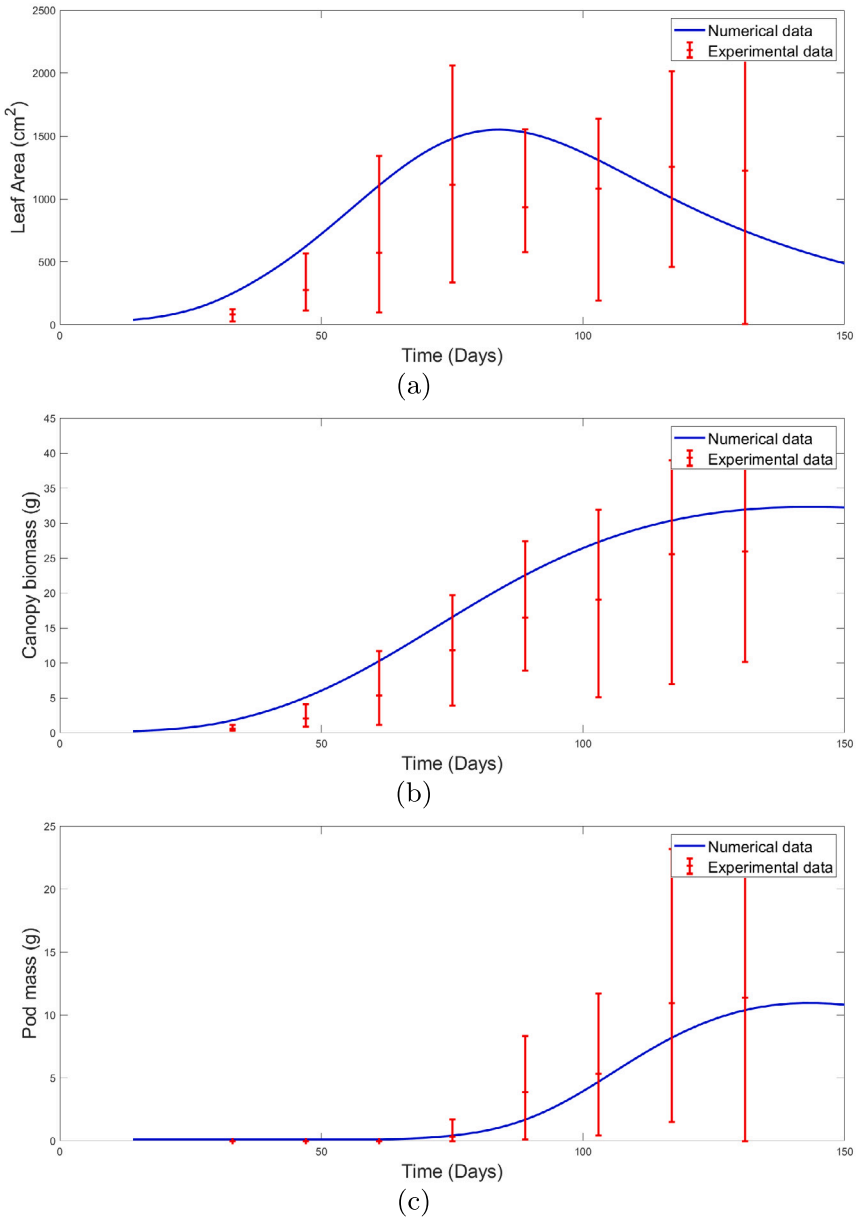

Fig. A.19. The simulated (a) leaf area, (b) canopy biomass and (c) pod mass compared with the experimental data for the species S19-3, using the data-fitted case of a temperature of 28 °C. Red bars indicate the upper and lower bounds of the experimental data.

There is some considerable amount of variation to be seen in leaf area, canopy biomass and pod mass with random variation of 10% to plant parameters. It can be seen that this variation generally causes a decrease in leaf area, canopy biomass and pod mass. The driver of this variation is the differences to plant height and the size of ground cover and it is clear that the system is especially sensitive to these parameters (see Fig. 17).

Our results show that the system is particularly impacted by variation in plant height. If all plants are the same height, then all plants experience the incurred competition equally. If plants differ in height then some plants will experience considerable competition and others none at all. Each set of randomly selected parameters will impact which plants experience competition. When coupled with the impact that plant position has on competition, we find that the impact of height is considerable.

In regards to ground cover, it can be seen that small changes in α_G, b_g and c_g exhibit large changes to yield. It can then be inferred that variation up to 10% is too large to accurately describe the experimental data. It must be stipulated however that the experimental data considers a much smaller sample size than what would be found in the field.

If random variation is removed from parameters ascertaining to height and ground cover growth rates, then we see a considerable decrease in overall variation, however we still see a decrease to overall plant yield. This is because at this fixed planting distance changes in parameter are more likely to have a detrimental effect on yield than a positive effect; this is summarised in Table 6. In the majority of cases, a tenfold change in parameter that increases yield causes a smaller change than the reciprocal change.

To understand the interplay between competition and random variation of plant parameters, we ran the simulation 100 times for using the default planting arrangement and again with planting distances increased tenfold. The resulting histograms are shown in Fig. 18. There is a clear increase in yield when planting distance is increased, with an average yield of 373.2 g using the default planting distance compared

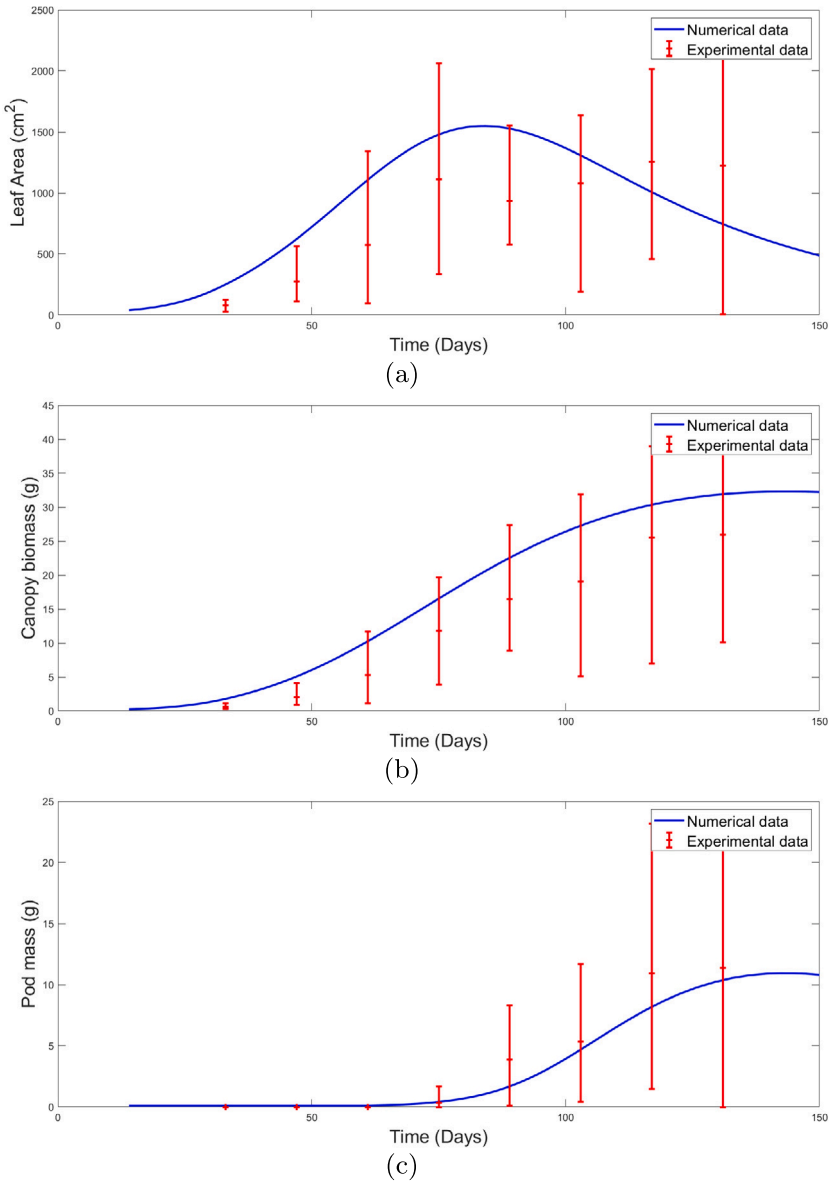

Fig. A.20. The simulated (a) leaf area, (b) canopy biomass and (c) pod mass compared with the experimental data for the species S19-3, using the non data-fitted case of a temperature of 23 °C. Red bars indicate the upper and lower bounds of the experimental data.

to 1703.2 g when planting distance is increased. We can also see that for decreased planting density the distribution is narrower and appears more 'normal', meaning that without the confounding affect of competition yield is more predictable.

8. Summary and conclusions

The purpose of this work was to develop a multi-scale mathematical model of bambara groundnut development that takes account of canopy–canopy competition for light in the context of glass-house growth. The model combines ODE's describing the height, leaf area, canopy biomass, canopy size and yield of each individual plant with that of an agent based approach used to specify plant position. Of particular importance in this modelling approach was modelling the plant ground cover and the overlap between neighbouring plants as this is fundamental for describing competition for light.

In this model overlap affects the maximum leaf area growth rate, the maximum ground cover growth rate via the leaf area term, the window of peak ground cover spreading, the growth rate of canopy biomass and the carrying capacity of canopy biomass. The plant canopy is assumed symmetrical and the presence of overlap prevents a plant from growing unencumbered into a space occupied by another plant. It would be an interesting addition to the model to consider asymmetry in the plant spreading. Then, a plant that is unable to spread in one direction, may continue to spread in another. This investigation is beyond the scope of this work, however would be an interesting area of further investigation.

In other crop models it is common to include competition in the form of a density factor that decreases growth as a proportion of the planting density. This approach can provide a reasonable prediction of yield, however it does not provide the full story. The approach described in this paper provides an insight into the effect that plant position, arrangement and varying planting distances have on the total crop yield. Additionally, parameterising a density factor can be difficult as it requires multiple studies to provide a realistic estimate. Modelling competition by modelling plant canopy size can be parameterised using fewer studies comprising of multiple plants.

To calibrate the model, additional data was required. This led to the design and completion of additional glasshouse experiments. By

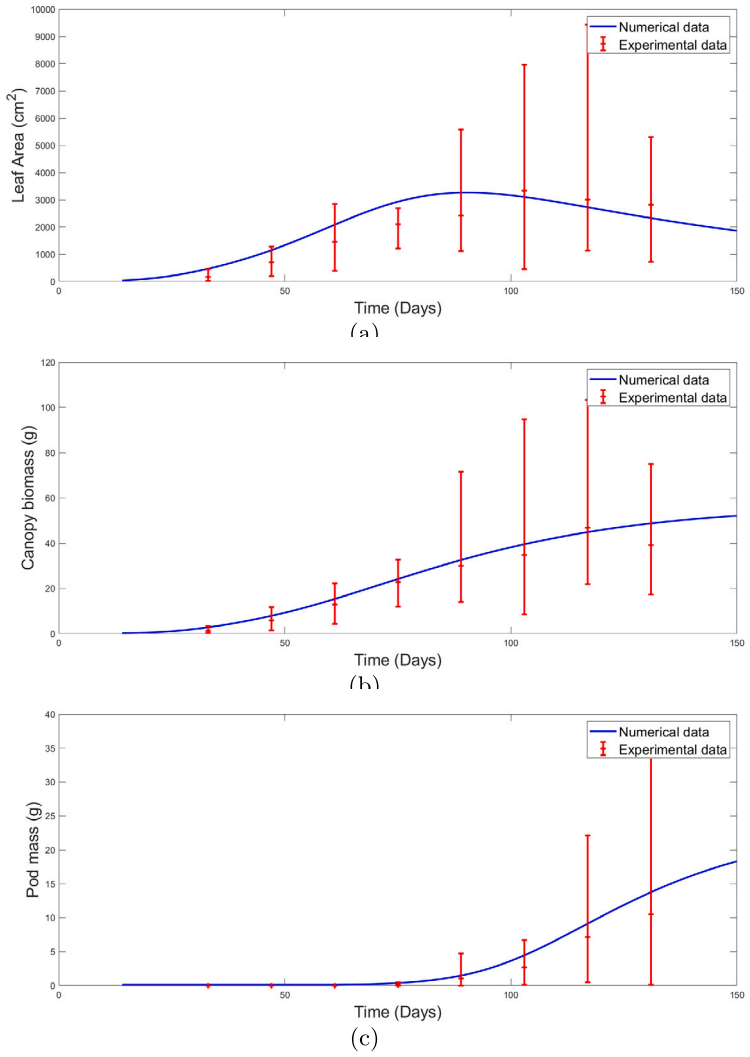

Fig. A.21. The simulated (a) leaf area, (b) canopy biomass and (c) pod mass compared with the experimental data for the species S19-3, using the non data-fitted case of a temperature of 33 °C. Red bars indicate the upper and lower bounds of the experimental data.

providing a more accurate insight into the size of the canopy, a more thorough picture of canopy–canopy interactions was attained. Individual plants are modelled as discs on a raised central stem. This approach allows for a tractable calculation that describes the general physiology of the plant. The model was evaluated against experimental data and it was demonstrated, that with this simple approach to modelling plant physiology, a good likeness to the real plant behaviour was achieved; the simulated data being within the upper and lower bounds of the observed glasshouse data.

Our agent based approach describes plant growth at the single plant level. By doing so, the mathematical model can be used to investigate the impact of individual plant physiology and planting in relation to other plants on the overall crop yield. As mentioned above, this includes different arrangements and planting distance; but also by modelling plant growth in terms of its phenomenological components it is possible to determine how individual plant parameters affect yield and therefore give insight into the effect of genetic diversity. Whilst phenomenological in nature, the multiscale framework introduced here is ripe for including further detailed processes at the sub-plant scale describing, for instance sub-cellular protein–protein interaction cascades and how these affect plant growth and development as well as inter-plant competition.

It was found that plant position has considerable impact on its growth. Predictably, plants on the corners of the plot area give the highest yield as they experience the least competition by neighbours. This is followed by plants along the edge and then the interior plants. Plant layout has a considerable impact on plants also, it was found that a circular arrangement gave the highest yield per plant, but since this layout allowed fewer plants to fit into the plot area, there was a smaller yield overall. Indented Grid 2 gave the largest overall crop yield.

Genetic diversity, modelled by including random variation in model parameter values, caused a decrease to overall yield. This is because increases in parameters that can potentially increase the yield also increase the competition between plants. If planting distance was to increase this would not necessarily continue to be the case. This insight is particularly relevant to underutilised crops, such as bambara groundnut, as comparatively large amounts of variation exists between plants.

In conclusion, this novel approach has been able to provide insight into how the qualities of individual plants have on the total crop. This is counter to the common approach of averaging plants properties over the many plant crop scale. It has been found that modelling with the inclusion of variation between plants indicates that a larger planting distance is more appropriate to increase yield. This conclusion could not have been drawn if all plant parameters were treated as identical.

CRediT authorship contribution statement

Josie Dodd: Undertook research, Developed code, Drafted manuscript. **Peter K. Sweby:** Supervision, Reviewed draft of manuscript. **Sean Mayes:** Conceptualised research, Provided supervision, Drafted manuscript. **Erik H. Murchie:** Supervision, Reviewed draft of manuscript. **Asha S. Karunaratne:** Supervision, Reviewed draft of manuscript, Provided experimental data. **Festo Massawe:** Supervision, Reviewed draft of manuscript. **Marcus J. Tindall:** Conceptualised research, Provided supervision, Drafted manuscript.

Declaration of competing interest

The authors declare that they have no known competing financial interests or personal relationships that could have appeared to influence the work reported in this paper.

Availability of data

Provided in manuscript.

Funding

Work was funded by Engineering and Physical Science Research Council (EPSRC grant EP/L505043/1) and Crops For the Future, Malaysia. **Availability of code**: Code can be made available on request.

Appendix. Supplementary information

We now compare the mathematical model described by Eqs. (41) to (45) to greenhouse data for S19–3 as described in Section 5. For these comparisons a crop of 9 plants were arranged in the layout illustrated in Fig. 5(a). Parameters for all plants were considered equal, the only difference between plants being the overlap incurred by their position. Simulated leaf area, canopy biomass and pod mass were averaged over all N plants and compared to the corresponding mean average of the experimental data. Temperature was constant for each simulation and a range of temperatures were investigated, corresponding to those in the TCRU experiments (23 °C, 28 °C and 33 °C).

A simulation of leaf area, canopy biomass and pod mass compared to experimental data for S19–3 at 28 °C is shown in Fig. A.19. This is the data set used to fit the model parameters for S19-3 and is hereby referred to as the 'fitting case'. The two non-fitted cases of 23 °C and 33 °C are given in Figs. A.20 and A.21, respectively. There is no experimental data for ground cover and so no visual fits are available.

The simulations of S19-3 show a good fit to the experimental data for all three temperatures, with the average pod mass being within the minimum and maximum of the experimental data for all 8 time points.

References

Aggarwal, P.K., Kalra, N., 1994. Analyzing the limitations set by climatic factors, genotype, water and nitrogen availability on productivity of wheat: II climatically potential yield and management strategies. Field Crop Res. 38, 93–103.

Aliyu, S., Massawe, F., Mayes, S., 2015. Beyond landraces: developing improved germplasm resources for underutilized species - a case for Bambara groundnut. Biotechnol. Genet. Eng. Rev. 30 (2), 127–141.

Alm, D.M., Pike, D.R., Hesketh, J.D., Stoller, E.W., 1988. Leaf area development in some crop and weed species. Biotronics: Environ. Control Environ. Biol. 17, 29–39.

Alshareef, I., 2010. The Effect of Temperature and Drought Stress on Bambara Groundnut (*Vigna Subterranea* (L.) Verdc) Landraces (Ph.D. thesis). University of Nottingham, U.K.

Azam-Ali, S.N., Sesay, A., Karikari, K.S., Massawe, F.J., Aguilar-Manjarrez, J., Bannayan, M., Hampson, K.J., 2001. Assessing the potential of an underutiized crop - a case study using bambara groundnut. J. Explor. Agric. 37, 433–472.

Bauer, S., Berger, U., Hildenbrandt, H., Grimm, V., 2002. Cyclic dynamics in simulated plant populations. Proc. R. Soc. Lond. Ser. B Biol. Sci. 269, 2443–2450.

Brink, M., Sibuga, K.P., Tarimo, A.J.P., Ramolemana, G.M., 1999. Quantifying photothermal influence on reproductive development in bambara groundnut (*Vigna subterranea*): models and their validation. Field Crop Res. Res. 66, 1–14.

Burgess, A.J., Retkute, R., Pound, M.P., Preston, S.P., Pridmore, T.P., Foulkes, J., Jensen, O., Murchie, E.H., 2015. High-resolution 3D structural data quantifies the impact of photoinhibition on long term carbon gain in wheat canopies in the field. Plant Physiol. 169, 1192–1204.

Cieslak, M., Seleznyova, A., Prusinkiewicz, P., Hanan, J., 2011. Towards aspect-oriented functional-structural plant modelling. Ann. Botany 108, 1025–1041.

Cornelissen, R.L.E.J., 2005. Modelling Variation in the Physiology of Bambara Groundnut (Ph.D. thesis). Cranfield University at Silsoe, U.K.

Cournede, P.H., Mathieu, A., Houllier, F., Barthelemy, D., De Reffye, P., 2008. Computing competition for light in the GREENLAB model of plant growth: A contribution to the study of the effects of density on resource acquisition and architectural development. Ann. Botany 101, 12071219.

de Wit, C.T., 1965. Photosynthesis of leaf canopies. In: Agriculture Research Reports, Vol. 663. Center for Agriculture Publication and Documentation, p. 57.

Esnal, A.R., Lopez-Fernandez, M.L., 2010. Modelling leaf development in Oxalis latifolia. Span. J. Agric. Res. 1695–1971–X.

Fourcaud, T., Zhang, X., Stokes, A., Lambers, H., Korner, C., 2008. Plant growth modelling and applications: The increasing importance of plant architecture in growth models. Ann. Botany 101 (8), 1053–1063.

Gaudio, N., Louarn, G., Barillot, R., Meunier, C., Vezy, R., Launay, M., 2021. Exploring complementarities between modelling approaches that enable upscaling from plant community functioning to ecosystem services as a way to support agroecological transition. In: Silico Plants 2021. diab037. http://dx.doi.org/10.1093/insilicoplants/diab037.

Godin, C., 1999. Representing and encoding plant architecture: A review. Ann. Forest Sci. 57, 413–438.

Godin, C., Caraglio, Y., 1997. A multiscale model of plant topological structures. J. Theoret. Biol. 191, 1–46.

Goudriaan, J., Van Laar, H.H., 1994. Modelling Potential Crop Growth Processes. Kluwer Academic Publishers, Dordrecht, p. 1.

Gramig, G., Stoltenberg, D., 2007. Leaf appearance base temperature and phyllochron for common grass and broadleaf weed species. Week Technol. 21, 249–254.

Granier, C., Massonnet, C., Turc, O., Muller, B., Chenu, K., Tardieu, F., 2002. Individual leaf development in *Arabidopsis thaliana*: a stable thermal-time-based programme. Ann. Botany 89, 595–604.

Hammer, G.L., Kropff, M.j., Sinclair, T.R., Porter, J.R., 2002. Future contributions of crop modelling - from heuristics and supporting decision making to understanding genetic regulation and aiding crop improvement. Eur. J. Agron. 18 (1–2), 15–31.

Karunaratne, A.S., 2009. Modelling the Response of Bambara Groundnut (*Vigna Subterranea (L.) Verdc*) for Abiotic Stress (Ph.D. thesis). University of Nottingham, U.K.

Karunaratne, A.S., Azam-Ali, S.N., Crout, M.J., 2011. Bamgro: A simple model to simulate the response of bambara groundnut to abiotic stress. Exp. Agric. 47, 489–507. http://dx.doi.org/10.1017/S0014479711000093, Cambridge University Press.

Li, T., Feng, Y., Li, X., 2009. Predicting crop growth under different cropping and fertilizing management practices. Agricult. Forest Meteorol. 149, 985–998.

Linnemann, A.R., Azam-Ali, S., 1993. Bambara groundnut (*Vigna subterranea*). In: Williams, J.T. (Ed.), Underutilized Crops: Pulses and Vegetables. Chapman and Hall, London, pp. 13–57.

Ma, Y.T., Wubs, A.M., Mathieu, A., Heuvelink, E., Zhu, J.Y., Hu, B.G., Cournede, P.H., de Reffye, P., 2010. Simulation of fruit-set and trophic competition and optimization of yield advantages in six *Capsicum* cultivars using functional-structural plant modelling. Ann. Botany 107 (5), 793–803.

Mabhaudhi, T., Modi, A., 2013. Growth, phenological and yield responses of a bambara groundnut (*Vigna subterranea (L.) Verdc.*) landrace to imposed water stress under field conditions. South Afr. J. Plant Soil 30 (2), 69–79.

Marcelis, L.F.M., Heuvelink, E., Goudriaan, J., 1998. Modelling biomass production and yield of horticultual crops: a review. Sci. Horticult. 74, 83–111.

Met office, 2016. [online] Available at: http://www.metoffice.gov.uk/renewables/solar [Accessed 28 June 2016].

Mkandawire, C., 2007. Review of bambara groundnut (*Vigna subterranea* (l.) verdc.) production in Sub-Sahara Africa. MedWell Agric. J. 2 (4), 464–470.

Monteith, J.L., Gregory, P.J., Marshall, B., Ong, C.K., Saffell, R.A., Squire, G.R., 1980. Physical measurements in crop physiology in growth and gas exchange. Exp. Agric. 17, 113–126.

Mwale, S.S., Azam-Ali, S.N., Massawe, F.J., 2007. Growth and development of bambara groundnut (*Vigna subterranea*) in response to soil moisture: 1. Dry matter and yield. Eur. J. Agron. 26, 345–353.

Nash, J.E., Sutcliffe, J.V., 1970. River flow forcasting through conceptiual models: Part I-A discussion of principles. J. Hydrol. 10, 282–290.

Schneider, M., Law, R., Illian, J.B., 2006. Quantification of neighbourhood-dependent plant growth by Bayesian hierarchical modelling. J. Ecol. 94, 310–321.

Summerfield, R.J., Roberts, E.H., Ellis, R.H., Lawn, R.J., 1991. Towards the reliable prediction of time to flowering in six annual crops. I. The development of simple models for fluctuating field environments. Exp. Agric. 27, 11–31.

Yan, H., Kang, M., Reffye, P., Dingkuhn, M., 2004. A dynamic, architectural plant model simulating resource-dependent growth. Ann. Botany 93, 591–602.

Zhang, B., DeAngelis, L., 2020. An overview of agent-based models in plant biology and ecology. Ann. Botany 126, 539–557.